III. 研究成果の刊行物・別刷

Author's Choice

THE JOURNAL OF BIOLOGICAL CHEMISTRY VOL. 285, NO. 33, pp. 25185–25195, August 13, 2010

Uncoating of Human Immunodeficiency Virus Type 1 Requires Prolyl Isomerase Pin1*[S]

Received for publication, February 16, 2010, and in revised form, May 26, 2010 Published, JBC Papers in Press, June 7, 2010, DOI 10.1074/jbc.M110.114256

Shogo Misumi[‡1,2], **Mutsumi Inoue**[‡1,3], **Takeo Dochi**[‡], **Naoki Kishimoto**[‡], **Naomi Hasegawa**[‡], **Nobutoki Takamune**[‡], **and Shozo Shoji**[‡§]

From the [‡]*Department of Pharmaceutical Biochemistry, Faculty of Medical and Pharmaceutical Sciences, Kumamoto University, Kumamoto 862-0973, Japan and* [§]*Kumamoto Health Science University, Kumamoto 861-5598, Japan*

The process by which the human immunodeficiency virus type 1 (HIV-1) conical core dissociates is called uncoating, but not much is known about this process. Here, we show that the uncoating process requires the interaction of the capsid (CA) protein with the peptidyl-prolyl isomerase Pin1 that specifically recognizes the phosphorylated serine/threonine residue followed by proline. We found that the HIV-1 core is composed of some isoforms of the CA protein with different isoelectric points, and one isoform is preferentially phosphorylated in the Ser^{16}-Pro^{17} motif. The mutant virus S16A/P17A shows a severely attenuated HIV-1 replication and an impaired reverse transcription. The S16A/P17A change increased the amount of particulate CA cores in the cytosol of target cells and correlated with the restriction of HIV-1 infection. Glutathione *S*-transferase pulldown assays demonstrated a direct interaction between Pin1 and the HIV-1 core via the Ser^{16}-Pro^{17} motif. Suppression of Pin1 expression by RNA interference in a target cell results in an attenuated HIV-1 replication and increases the amount of particulate CA cores in the cytosol of target cells. Furthermore, heat-inactivated, inhibitor-treated, or W34A/K63A Pin1 causes an attenuated *in vitro* uncoating of the HIV-1 core. The Pin1-dependent uncoating is inhibited by antisera raised against a CA peptide phosphorylated at Ser^{16} or treatment of the HIV-1 core with alkaline phosphatase. These findings provide insights into this obscure uncoating process in the HIV-1 life cycle and a new cellular target for HIV-1 drug development.

The HIV-1[4] CA protein must assemble properly and should be sufficiently stable to protect the genomic RNA but must disassemble to allow genomic RNA release after fusion. Because both the assembly and disassembly processes cannot act on the CA proteins at the same time, an important question concerns the mechanisms responsible for the switch from the assembly to disassembly mode. However, not much has been known about the disassembly process so far because this process has been assumed to occur immediately after fusion (1, 2).

Recent studies suggested that cell factors may assist the disassembly process, commonly referred to as uncoating (3, 4). Cellular activation has long been considered a requirement for HIV-1 infection of CD4$^+$ T cells, because HIV-1 fails to infect resting CD4$^+$ T cells from peripheral blood. Infection is aborted either during reverse transcription (5) or before nuclear import of the viral preintegration complex (6). It was shown that HIV-1 can enter resting CD4$^+$ T cells efficiently, but only short incomplete reverse transcripts are formed. Auewarakul *et al.* (3) demonstrated that the uncoating of HIV-1 is efficiently induced by lysate from activated CD4$^+$ lymphocytes, whereas resting CD4$^+$ lymphocyte lysate cannot uncoat the HIV-1 core. Furthermore, Warrilow *et al.* (4) reported that endogenous reverse transcription is inefficient in comparison with reverse transcription in cell infection, as exemplified by the poor efficiency of the production of intravirion late reverse transcription products. This observation also suggests a requirement for a contribution from the host cell environment for optimal HIV-1 reverse transcription to proceed by an ordered disassembly of the HIV-1 CA core. These findings suggest that the uncoating activity that releases the CA protein from the HIV-1 core is due to cellular factors.

We previously reported that the HIV-1 core is composed of some isoforms of the CA protein with different isoelectric points (7). The difference in isoelectric points among CA protein isoforms might be due to multiple post-translational modifications, such as phosphorylation. Indeed, several reports have provided evidence that the CA protein is predominantly phosphorylated at serine residues rather than threonine/tyrosine residues (8, 9). Phosphorylation often plays an important role in modulating protein activity and protein-protein interactions and promoting the disassembly of cellular macromolecular assembly such as the nuclear pore complex. Protein kinases catalyze post-translational phosphorylation, and many kinases are themselves regulated by phosphorylation. The phosphor-

* This work was supported in part by a Grant-in-Aid for Scientific Research from the Ministry of Education, Culture, Sports, Science, and Technology of Japan and a Health Science Research Grant from the Ministry of Health, Labour, and Welfare of Japan.

Author's Choice—Final version full access.

[S] The on-line version of this article (available at http://www.jbc.org) contains supplemental Table S1 and Figs. S1–S5.

[1] Both authors contributed equally to this work.

[2] To whom correspondence should be addressed: Kumamoto University, Dept. of Pharmaceutical Biochemistry, Faculty of Medical and Pharmaceutical Sciences, 5-1 Oe-Honmachi, Kumamoto 862-0973, Japan. Tel.: 81-96-371-4362; Fax: 81-96-362-7800; E-mail: misumi@gpo.kumamoto-u.ac.jp.

[3] Recipient of Japan Society for the Promotion of Science for Young Scientists Research Fellowship 217212.

[4] The abbreviations used are: HIV-1, human immunodeficiency virus type 1; CA, capsid; GST, glutathione *S*-transferase; CPE, cytopathic effect; ALP, alkaline phosphatase; RT, reverse transcriptase; PBS, phosphate-buffered saline; CBB, Coomassie Brilliant Blue; MALDI-TOF, matrix-assisted laser desorption ionization time-of-flight; KLH, keyhole limpet hemocyanin; ELISA, enzyme-linked immunosorbent assay; WT, wild type; mAb, monoclonal antibody; siRNA, small interfering RNA; RPDE, relative percentage of disassembly efficiency; MA, matrix; SIV, simian immunodeficiency virus.

ylation-dependent modulation of protein-protein interactions is the pivotal molecular switch for the regulation of signaling processes within eukaryotic cells. Furthermore, current studies point toward mitotic phosphorylation of nucleoporins as the trigger of the nuclear pore complex disassembly process (10–12). These findings led to a hypothesis that phosphorylation induces the dissociation of CA-CA protein interactions and promotes the disassembly of the HIV-1 core.

In this study, we show that the serine residue in the Ser[16]-Pro[17] motif of a CA protein isoform is phosphorylated and that peptidyl-prolyl isomerase Pin1 specifically recognizes the Ser[16]-Pro[17] motif of the HIV-1 core. Furthermore, we demonstrated that Pin1 prolyl isomerase activity is required for the disassembly of the HIV-1 core. These results reveal a novel regulation step of HIV-1 infection.

EXPERIMENTAL PROCEDURES

Virus Preparation—HIV-1_{LAV-1} and HIV-1_{JRFL} were prepared as previously described (7, 13). The supernatant from the culture medium of CEM/LAV-1 or CEM-CCR5/JRFL was filtered through a 0.22-μm-pore size disposable filter and then centrifuged at 43,000 × *g* for 3 h at 4 °C. The obtained pellet was resuspended in PBS(−) (0.02% KH_2PO_4, 0.29% $Na_2HPO_4 \cdot 12H_2O$, 0.8% NaCl, 0.02% KCl) and then centrifuged at 100,000 × *g* for 1 h at 4 °C. The resulting pellet was resuspended in 10 mM Tris-HCl buffer (pH 8.0). Virions were treated with or without 1 mg/ml subtilisin (ICN Biomedicals Inc., Costa Mesa, CA) in 10 mM Tris-HCl (pH 8.0) and 1 mM EDTA-2Na. The virions were then purified using PBS(−) by column chromatography with a 10-ml column of Sepharose CL-4B™ at room temperature in a biosafety hood. Fractions containing the virus were pooled and centrifuged at 100,000 × *g* for 1 h at 4 °C. The resulting pellet derived from HIV-1_{LAV-1} or HIV-1_{JRFL} was boiled for 1 min and lysed in 200 μl of lysis buffer (9.5 M urea, 2% (w/v) Nonidet P-40, 2% ampholine (pH 6–8), and 5% 2-mercaptoethanol). For the MAGIC-5 assay and quantitative analysis of HIV-1 reverse transcription, pNL4-3-based mutants and replication-defective viruses were prepared as follows. The HIV-1 proviral DNA constructs pNL4-3 (14), containing full-length HIV-1, and pNL4-3Δenv, in which there is a truncation in *env*, were the control viruses utilized in this study. The 1136-bp fragment containing the BssHII and SpeI sites of pNL4-3 or pNL4-3Δenv was subcloned into pT7Blue (Novagen, Inc., Madison, WI). Point mutations were introduced into the Ser[16]-Pro[17] motif in the HIV_{NL4-3} or $HIV_{NL4-3\Delta env}$ CA protein by site-directed mutagenesis. The fragments were sequenced to confirm mutations. The mutant BssHII-SpeI fragment was recloned into the full-length HIV expression plasmid $pNL4\text{-}3_{BssHII\text{-}SpeI}$ or $pNL4\text{-}3\Delta env_{BssHII\text{-}SpeI}$, which does not have the backbone BssHII-SpeI fragment. All of the mutations were verified by sequencing. The mutant viruses ($HIV_{NL4-3(S16A/P17A)}$, $HIV_{NL4-3\Delta envWT}$, and $HIV_{NL4-3\Delta env(S16A/P17A)}$) were produced by the transient transfection of HEK293 cells using pNL4-3(S16A/P17A) or pNL4-3Δenv and pNL4-3Δenv(S16A/P17A) with the pNL4-3-based env expression vector. Four days after transfection, the virus-containing supernatant was collected and clarified by filtration through 0.45-μm-pore size filters. Virus production and release were monitored by measuring virion-associated RT activity as previously described (7).

Peptide Mass Fingerprinting—An aliquot of the viral lysate was subjected to two-dimensional polyacrylamide gel electrophoresis in accordance with the method of O'Farrell (15). The sample was loaded using a 15-cm immobilized pH gradient tube gel (pH 6–8) (Daiichi Pure Chemicals Co., Ltd.). The proteins were focused for 1 h at 400 V followed by a step gradient (1000 V for 18 h; 2000 V for 1 h). After the second-dimensional run (10–20% PAG large gel; Daiichi Pure Chemicals Co., Ltd.), the gel was stained with Coomassie Brilliant Blue (CBB) R-250 or ProQ diamond (Invitrogen). CBB-stained gel pieces were excised from the gel and immersed in 100 μl of acetonitrile, dried under vacuum centrifugation, rehydrated in 25 μl of trypsin solution (3.9 ng/μl trypsin in 170 mM ammonium bicarbonate, 40% $H_2{}^{18}O$, 30% acetonitrile) or 25 μl of Glu-C solution (10 ng/μl Glu-C in 55 mM NaH_2PO_4 and 40% $H_2{}^{18}O$), and then incubated for 60 min. The unabsorbed enzyme solution was removed, and the gel pieces were incubated for 12 h at 37 °C. The digested peptides were purified using ZipTip (Nihon Millipore Ltd., Tokyo, Japan) and then analyzed by MALDI-TOF mass spectrometry as previously described (7). Phosphorylated peptides were analyzed as follows. Alkaline phosphatase (Wako Pure Chemical Industries, Ltd.) liberated the phosphate group from phosphorylated peptides. Alkaline phosphatase reactions were carried out directly on the MALDI target. The sample was mixed with 12 ng/ml ALP from *Escherichia coli* (Wako Pure Chemical Industries) that had been dissolved in 10 mM ammonium bicarbonate. The reactions were carried out for 5 min at room temperature followed by the addition of 0.5 μl of α-cyano-4-cinnamic acid or 2,5-dihydroxybenzoic acid saturated in 40% acetonitrile, 0.1% trifluoroacetic acid.

Preparation of HIV-1 p24-derived Peptide-Keyhole Limpet Hemocyanin (KLH) Conjugates and Antibody Screening—A p24-derived linear decapeptide (pSP, H_2N-HQAIpSPRTLN-COOH) was synthesized using an automatic peptide synthesizer. The molecular mass was determined by MALDI-TOF mass spectrometry (Burker Franzen Analytik). The amino group of His^1 was coupled to KLH (pSP-KLH) through bis(sulfosuccinimidyl)suberate (Thermo Fisher Scientific Inc.). Ten BALB/c mice were immunized intraperitoneally with 200 μg of pSP-KLH in Freund's adjuvant at 1-week intervals and administered an intravenous boost of 40 μg of pSP-KLH 3 days prior to splenectomy. The blood samples were collected prior to euthanasia and centrifuged at 1500 × *g* for 5 min, and the anti-pS16/P17 serum was harvested. Then the mice were euthanized, and their spleens were removed for *in vitro* hybridoma cell production. The hybridomas were generated by a standard method, by which splenocytes were fused with P3U1 cells and selected in hypoxanthine-, aminopterin-, and thymidine-supplemented media. In the screening, supernatants were tested for reactivity to ELISA plates coated with pSP. The hybridoma that produced high titers of anti-pS16/P17 mAb (3/D-6) was then cloned.

Preparation of HIV-1 CA Cores and Detection of Phosphorylated CA Protein in the HIV Core—The WT HIV CA cores were purified in accordance with the method of Auewarakul *et al.* (3) with some modifications. Briefly, 3 ml of purified cell-free viruses was overlayered on a discontinuous sucrose density gra-

dient. The gradient was composed of 1 ml of 50% sucrose at the bottom and 1 ml of 10% sucrose containing 0.1% Igepal CA-630 on the top. The overlayered gradient was then centrifuged at 100,000 × *g* in a Swing Rotor P65ST (HitachiKoki Co., Ltd.) for 2 h at 4 °C. The pellets containing viral cores were then resuspended in the uncoating assay buffer (50 mM NaH_2PO_4, pH 7.2, 150 mM NaCl, and 200 μM sodium orthovanadate) and pooled. The CA cores were quantitated by measuring HIV-1 p24 antigen with RETRO-TEK HIV-1 p24 antigen ELISA (ZeptoMetrix Corp.). To examine the Ser^{16} phosphorylation of CA core, the pellets containing viral cores were then lysed with 62.5 mM Tris-HCl, 2% SDS, 10% glycerol (pH 6.8), and 10% 2-mercaptoethanol. The lysate from HIV cores was subjected to SDS-PAGE, and separated products were transferred to a polyvinylidene difluoride membrane for Western blotting. The membrane was stained with normal mouse serum and anti-pS16/P17 serum raised against pSP-KLH with or without pSP.

Viral Infectivity Assay—Jurkat and CEM cells (1 × 10^5) were exposed to the HEK293 cell-derived WT virus or S16A/P17A variant (100 ng of p24 antigen) for 2 h at 37 °C, washed with PBS(−), and cultured for 96 h. Virus infectivity was monitored by measurement of the p24 antigen from cell culture supernatants using RETRO-TEK HIV-1 p24 antigen ELISA (ZeptoMetrix Corp.).

Viral Entry Assay and Quantitative Analysis of HIV-1 Reverse Transcription during Acute Infection—The entry level of WT or mutant viruses was determined as follow. Viral entry assay was performed using the protocol of Kawano *et al.* (16) with modifications. MAGIC-5 cells (1 × 10^6 cells) were exposed to the virus (213.9 ng of HIV-1 RT) at 37 °C for 2 h. The cells were washed with PBS(−) and then incubated for 5 min at 37 °C in PBS(−) containing 0.25% trypsin. After trypsinization, the cells were washed twice with PBS(−) and pelleted. Cell-associated CA antigen content was determined by Western immunoblot analysis using an anti-p24 mAb (Immuno Diagnostics, Inc.). Furthermore, *de novo* synthesized HIV-1 cDNA was analyzed with or without Pin1 siRNA treatment in accordance with the method of Ikeda *et al.* (17).

Electron Microscopy of Virus—A viral preparation was fixed with 0.1 M sodium phosphate buffer (pH 7.4) containing 2% paraformaldehyde and 2.5% glutaraldehyde at 4 °C for 2 h prior to postfixation with 1% osmium tetroxide for 30 min at 4 °C. After dehydration in ethanol, the specimens were embedded in epoxy resin.

MAGIC-5 Assay and Cytopathic Effect (CPE) Assay—Viral infectivity was determined using MAGIC-5 cells as previously described in Ref. 18. MAGIC-5 cells (1 × 10^4 cells) were incubated in suspensions of WT, mutant, or single-round replication-defective viruses with 20 μg/ml DEAE dextran for 2 h and then cultured in a medium (200 μl) for 48 h. The cells were fixed, and HIV-1-infected cells identified by their blue staining were counted by conventional methods. To further examine whether a decrease in endogenous Pin1 expression level decreases viral infectivity, both MAGIC-5 assay and CPE assay were performed. 60 nM small interfering RNA against Pin1 (Pin1 C1 sense siRNA, GCCAUUUGAAGACGCCUCGdTdT; Pin1 C1 antisense siRNA, GAGGCGUCUUCAAAUGGCdTdT; Pin1 C2 sense siRNA, CUGGCCUCACAGUUCAGCGdTdT; Pin1 C2 antisense siRNA, CGCUGAACUGUGAGGCCAGdTdT; Pin1 C3 sense siRNA, GCCGAGUGUACUACUUCAAdTdT; or Pin1 C3 antisense siRNA, UUGAAGUAGUACACUCGGCdTdT) or control siRNA (sense siRNA against GL2 Luciferase, CGUACGCGGAAUACUUCGAdTdT; or antisense siRNA, UCGAAGUAUUCCGCGUACGdTdT) was transfected into the MAGIC-5 cells (1 × 10^4 or 2 × 10^5 cells) using Lipofectamine 2000. The cells were infected with HIV-1_{LAV-1} (12 ng of p24 antigen). HIV-1_{LAV-1}-infected cells identified by their blue staining were counted by conventional methods. In CPE assay, the cells were infected with a single-round replication-defective HIV-1 ($HIV_{NL4-3\Delta envWT}$, 11 ng of HIV RT).

Fate-of-Capsid Assay—Fate-of-capsid assay was performed in accordance with the method of Sodroski and co-workers (19) with some modifications. Briefly, recombinant HIV-1 virus-like particles (WT HIV-1(VSV-G) and S16A/P17A HIV-1(VSV-G)) were produced by cotransfection of 293T cells with pHCMV-G and pNL4-3Δenv or pNL4-3Δenv carrying the S16A/P17A mutation (pNL4-3Δenv(S16A/P17A)) as described in Ref. 20. To examine whether the infectivity defect of the S16A/P17A variant is linked to a dysfunction of uncoating, MAGIC-5 (4.5 × 10^6) cells were seeded in 60-cm^2 flasks and the next day incubated with either 5 ml of WT HIV-1(VSV-G) or 5 ml of S16A/P17A HIV-1(VSV-G) incubated at 37 °C for 4 h after 30 min of incubation at 4 °C. On the other hand, to examine whether Pin1 depletion is linked to a dysfunction of uncoating, MAGIC-5 cells (4.0 × 10^6) were transfected with Pin1 C1 and C2 siRNA (600 nM) or control siRNA (600 nM) using Neon™ transfection system (Invitrogen) and incubated for 44 h. The cells were further incubated with 5 ml of WT HIV-1(VSV-G) at 37 °C for 4 h after 30 min of incubation at 4 °C. These cells were washed three times with ice-cold PBS and detached by incubating with 2 ml of proteinase K (7 mg/ml in Dulbecco's modified Eagle's medium) for 5 min at 4 °C. The cells were washed once in Dulbecco's modified Eagle's medium containing 10% fetal bovine serum and twice in PBS. The pellets were resuspended in 2 ml of hypotonic lysis buffer (10 mM Tris-HCl, pH 8.0, 10 mM KCl, and 1 mM EDTA) and placed on ice for 15 min. The cells were lysed using a 7-ml Dounce homogenizer and 15 strokes with pestle B. Cell debris was removed by centrifugation for 3 min at 2,000 × *g*. After centrifugation, 1 ml of lysate was layered onto a 3.5-ml of 50% sucrose cushion (made in PBS) and centrifuged at 125,000 × *g* for 2 h at 4 °C in a Swing Rotor P65ST (HitachiKoki Co., Ltd). After centrifugation, 150 μl from the topmost part of the supernatant was collected and made 1× in SDS sample buffer. The pellets were resuspended in 10 μl of 1× SDS sample buffer. The samples were subjected to SDS-PAGE and Western blotting for CA proteins.

Determination of Pin1-CA Interaction—The interaction between Pin1 and the CA core was determined by GST-Pin1 pulldown assay. Recombinant Pin1 proteins were produced as N-terminal GST-tagged proteins as previously described (21). The CA core was treated with ALP (Wako Pure Chemical Industries) or heat-denatured ALP for 2 h (final concentration, 0.024 μg/μl ALP) in a buffer containing 50 mM NaH_2PO_4 (pH 7.2), 150 mM NaCl, 200 μM sodium orthovanadate, 10% glycerol, and 1% Triton X-100 and then incubated with 30 μl of beads containing GST or GST-Pin1 proteins for 2 h at 4 °C.

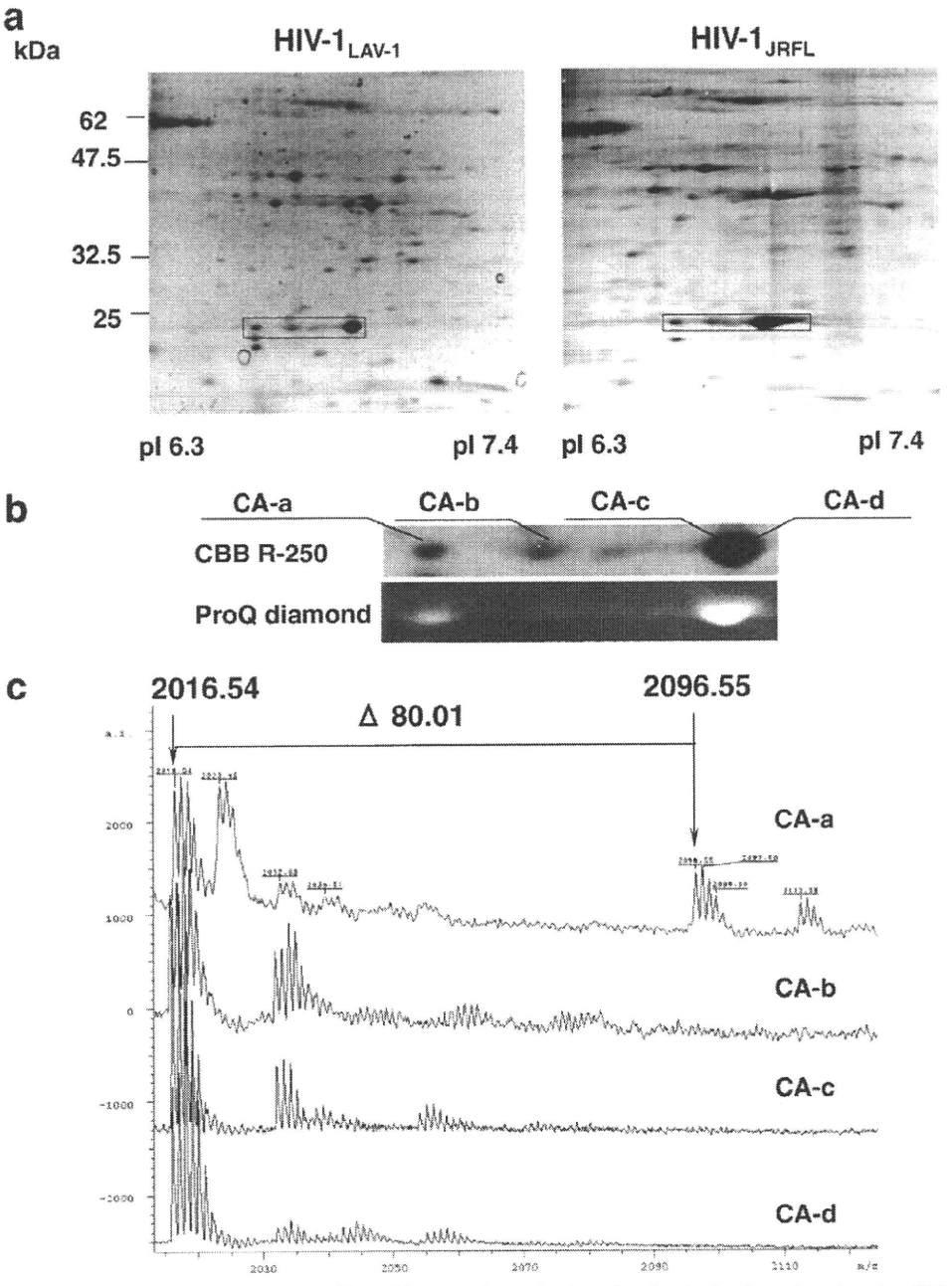

FIGURE 1. **A serine residue in the Ser[16]-Pro[17] motif of a CA isoform is selectively phosphorylated.** *a*, CBB R-250-stained two-dimensional gel images of HIV-1_{LAV-1} and HIV-1_{JRFL}. The *rectangles* indicate CA isoforms in virions. *b*, CBB R-250 and ProQ diamond staining of CA isoforms of HIV-1_{LAV-1}. *c*, spectra of *N*-terminal tryptic peptides derived from CA isoforms of HIV-1_{LAV-1}. The peak of $[M+H]^+$ at *m/z* 2096.55 corresponds to the phosphorylated form of the N-terminal tryptic peptide Pro_1-Arg_{18} of CA-a. *d*, liberation of phosphate group from N-terminal phosphorylated Pro_1-Arg_{18} derived from CA-a using alkaline phosphatase. The *lower* and *upper panels* show samples treated and not treated with alkaline phosphatase, respectively. The phosphorylated Pro_1-Arg_{18} disappeared after the phosphatase treatment. *e*, incorporation of phosphorylated CA-a into HIV core. The purified HIV core is subjected to Western immunoblot analysis using normal sera or anti-pS16/P17 serum with or without pSP, H_2N-HQAIpSPRTLN-COOH.

Immunoblotting analysis was performed using an anti-p24 mAb (Immuno Diagnostics, Inc.). Furthermore. a fraction of the ALP-treated CA core was subjected to Western blot analysis using an anti-pS16/P17 mAb raised against a synthetic phosphoserine-containing peptide, pSP, or an anti-p24 mAb.

Suppression of Pin1 Expression by siRNA—MAGIC-5 cells were transfected with Pin1 C3 siRNA (30–120 nM) or control siRNA (30–120 nM). The cells were infected with the WT virus and harvested 2 h after infection. To confirm the level of Pin1 expression, immunoblot analysis was carried out using the chemiluminescence protocol. The mouse monoclonal and goat polyclonal antibodies used were as follows: anti-Pin1 (R & D Systems, Inc.), anti-actin (Oncogene™ research product), and anti-lactate dehydrogenase (Chemicon) antibodies.

Uncoating Assay—The WT HIV CA core was purified as described above. The purified CA cores (2 ng) were resuspended in the uncoating assay buffer (50 mM NaH_2PO_4, pH 7.2, 150 mM NaCl, 200 μM sodium orthovanadate) and incubated with 0.114 μg/μl GST-Pin1, 0.114 μg/μl heat-denatured GST-Pin1, 0.114 μg/μl GST-Pin1 treated with juglone (molar ratio of GST-Pin1:juglone = 1:10; juglone was preincubated with GST-Pin1 at 37 °C for 1 h and then removed by gel filtration) or 0.114 μg/μl GST-Pin1(W34A/K63A) at 37 °C for 1 h. To examine whether the extent of CA disassembly was enhanced by Pin1, the pellets from the uncoating reactions were subjected to Western blot analysis using the anti-p24 mAb. Furthermore, a fraction of purified CA cores was pretreated with anti-pS16/P17 sera or normal sera. Another fraction of purified CA cores was treated with ALP (final concentration, 0.345 μg/μl) or heat-denatured ALP (final concentration, 0.345 μg/μl). The resulting CA cores were incubated with 0.114 μg/μl GST-Pin1 at 37 °C for 1 h. Each core suspension was then diluted in 5 ml of uncoating assay buffer and centrifuged at 100,000 × *g* for 2 h at 4 °C. The extent of CA release is quantified by p24 ELISA (ZeptoMetrix Corporation; the detection limit for the p24 antigen by ELISA was 7.8 pg/ml as provided by the manufacturer) because the undissociated cores were pelleted, and the dissociated CA protein was in the supernatant after ultracentrifugation. The relative percentage of disassembly efficiency (RPDE) is given by RPDE (%) = $100 \times (CA_S/CA_T)/(CA_{SC}/CA_{TC})$, where CA_S is the concentration of the CA protein in the supernatant, CA_T is the concentration of total CA protein in the supernatant plus pellet in the disassembly experiments of the CA core using boiled, juglone-treated

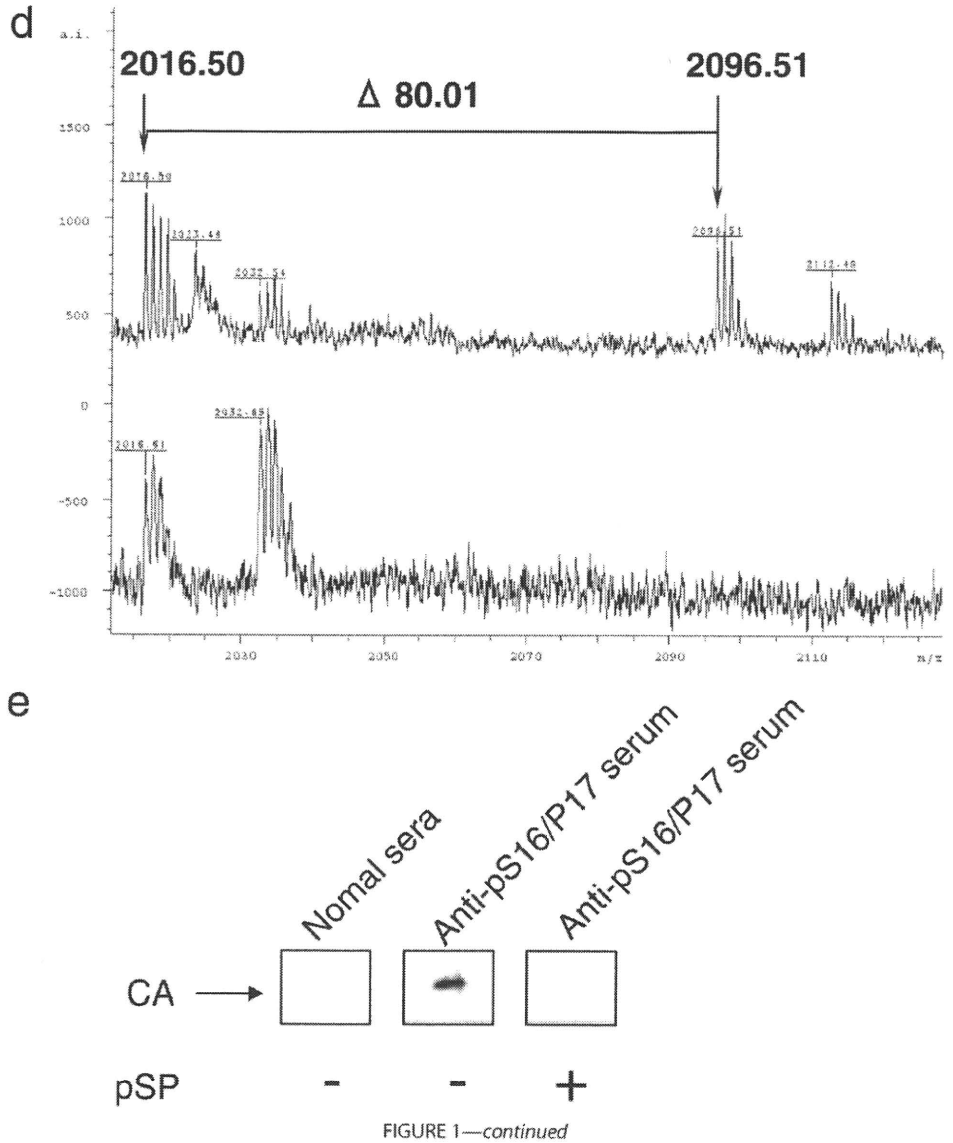

FIGURE 1—*continued*

GST-Pin1, or GST-Pin1(W34A/K63A); CA_{SC} is the concentration of the CA protein in the supernatant; and CA_{TC} is the concentration of total CA protein in the supernatant plus pellet in the control experiment using GST-Pin1. Likewise, the RPDE of CA cores pretreated with anti-pS16/P17 sera or ALP is given by RPDE (%) = $100 \times (CA_S/CA_T)/(CA_{SC}/CA_{TC})$, where CA_S is the concentration of CA protein in the supernatant; CA_T is the concentration of total CA protein in the supernatant plus pellet in the disassembly experiments of CA core pretreated with anti-pS16/P17 sera or ALP using the GST-Pin1; CA_{SC} is the concentration of CA protein in the supernatant; and CA_{TC} is the concentration of total CA protein in the supernatant plus pellet in the control experiments of CA core pretreated with normal mouse sera or heat-denatured ALP using the GST-Pin1.

RESULTS

A CA Protein Isoform Is Selectively Phosphorylated at Serine Residue 16 in the Ser[16]-Pro[17] Motif and Incorporated into the HIV Core—Some isoforms of the HIV-1 CA protein associated with CXCR4-tropic HIV-1_{LAV-1} or CCR5-tropic HIV-1_{JRFL} were identified by proteomics using two-dimensional gel electrophoresis and MALDI-TOF mass spectrometry (Fig. 1*a* and supplemental Table S1). We found that four isoforms of the HIV-1_{LAV-1} CA protein (CA-a (pI 6.70), CA-b (pI 6.80), CA-c (pI 6.91), and CA-d (pI 6.95)) are inside the virion (Fig. 1*b*). The differences between the pI values of the four isoforms of the CA protein may be due to post-translational modifications, such as phosphorylation and formylation (8, 9, 22, 23). Indeed, the CA proteins are composed of phosphorylated and unphosphorylated (Fig. 1*b*, *lower panel*) and formylated isoforms (23). Peptide mass fingerprinting data were used to identify the probable co/post-translational modifications. Then the specific phosphorylation of the N-terminal tryptic peptide ([1]PIVQNIQGQMVHQAISPR[18]) of CA-a was estimated because the spectrum corresponding to the N-terminal tryptic peptide exhibited a peak at *m/z* 2016.54 and the mass spectrum corresponding to the phosphorylated form exhibited a peak at *m/z* 2096.55 (Fig. 1*c*). The phosphorylation was confirmed by the liberation of a phosphate group from the N-terminal peptide of CA-a. The peak of $[M+H]^+$ at *m/z* 2016.50 corresponded to the peptide ([1]PIVQNIQGQMVHQAISPR[18]) whose phosphate group was cleaved off by an alkaline phosphatase (ALP) (Fig. 1*d*). These results show that the serine residue in the Ser^{16}-Pro^{17} motif of CA-a is selectively phosphorylated. To further determine whether CA-a is actually present in the CA core, the WT CA core was purified in accordance with the method of Auewarakul *et al.* (3) and was subjected to Western blot analysis using anti-pS16/P17 serum with or without pSP. As shown in Fig. 1*e*, CA-a is actually incorporated into the CA core.

Mutation at the Ser[16]-Pro[17] Motif Affects Uncoating Process—To study the role of the phosphorylated Ser^{16} that precedes Pro, we replaced Ser^{16} with glutamic acid (S16E) or alanine (S16A) to mimic phosphorylated or unphosphorylated Ser, respectively. We then tested the infectivity of the mutants by MAGIC-5 assay (21). The results showed that the S16E variant had the same infectivity as the wild type (Fig. 2*a*, *WT*). In contrast, the S16A variant had a decreased infectivity (Fig. 2*a*, $p < 0.01$). Assuming that glutamic acid mimics the negative charge of phosphorylated Ser^{16} in only a fraction of the CA protein in a viral core, the results obtained for S16E or S16A suggest that phosphorylation at Ser^{16} plays a critical role in maintaining

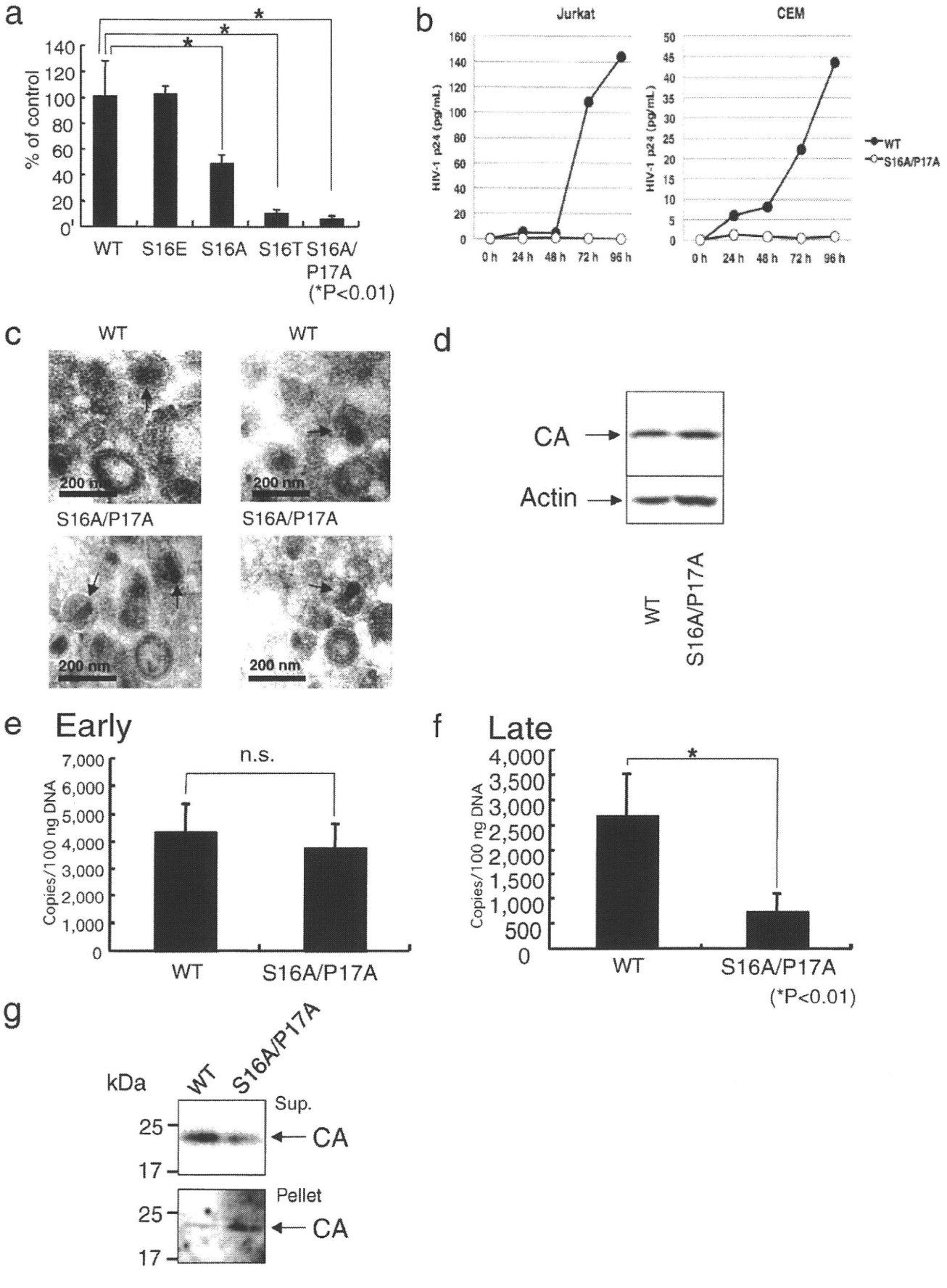
a
% of control
WT
S16E
S16A
S16T
S16A/P17A
(*P<0.01)
b
Jurkat
CEM
HIV-1 p24 (pg/mL)
0 h
24 h
48 h
72 h
96 h
WT
S16A/P17A
c
WT
WT
S16A/P17A
S16A/P17A
200 nm
d
CA
Actin
WT
S16A/P17A
e
Early
n.s.
Copies/100 ng DNA
WT
S16A/P17A
f
Late
*
Copies/100 ng DNA
WT
S16A/P17A
(*P<0.01)
g
kDa
WT
S16A/P17A
Sup.
CA
Pellet
CA
25
17

viral infectivity. To examine whether the phenotype of the S16A variant was specific to the selected amino acid changes, we produced another variant with a phosphorylatable amino acid residue, changing Ser to Thr (S16T). The S16T variant showed a remarkably decreased infectivity compared with the WT virus (Fig. 2*a*, $p < 0.01$), suggesting that the Ser^{16} residue in the highly conserved Ser^{16}-Pro^{17} motif (supplemental Fig. S1) plays an important role in maintaining the viral infectivity. To further investigate why Ser^{16} in a fraction of the CA protein in the virion needs to be phosphorylated, we generated another variant (S16A/P17A) because single-point mutations of Ser^{16} in the Ser^{16}-Pro^{17} motif may provide an alternate binding site for conventional peptidyl-prolyl *cis-trans* isomerases, such as cyclophilins, or FK-506-binding proteins, which catalyze the *cis-trans* isomerization of Xaa-Pro peptide bonds (where Xaa is the preceding amino acid) in oligopeptides or proteins. The S16A/P17A variant also had a markedly decreased infectivity in MAGIC-5 cells (Fig. 2*a*, $p < 0.01$) and could not replicate efficiently in T cell lines, Jurkat cells, and CEM cells (Fig. 2*b*), although the core yield of the S16A/P17A variant from HEK293 cells was very similar to that of WT HIV-1, and the phenotypes of the CA core were normal (Fig. 2*c*). Furthermore, to determine whether the lack of infectivity of S16A/P17A was due to a defect in the reverse transcription process, we carried out a viral entry assay and quantitative real time PCR analysis using primers designed to specifically amplify early or late products of reverse transcription. The viral entry assay indicated that the entry levels of S16A/P17A and WT were the same because the amounts of S16A/P17A CA protein in subcellular fractions were very similar to that of WT CA protein (Fig. 2*d*). However, compared with WT, S16A/P17A produced the same level of the early (R/U5) form of the viral cDNA product (Fig. 2*e*) but showed a significant decrease in the level of the late (R/gag) form of the viral cDNA product (Fig. 2*f*, $p < 0.01$). To further examine whether the infectivity defect of the S16A/P17A variant is linked to a dysfunction of uncoating, cell-based fate-of-capsid uncoating assay developed by Sodroski's group (19) was performed. This assay allows us to measure the amounts of cores and soluble free forms of the CA protein present in the cytosol of infected cells. Moreover, the appearance of CA cores in the cytosol inversely correlates with the proper conversion of CA cores to soluble CA in target cells. The amounts of pelletable CA cores in the cells infected with the S16A/P17A mutant virus increased against those detected in the cells infected with WT virus (Fig. 2*g*, *lower panel, Pellet*). Furthermore, the levels of the CA protein in the supernatants from MAGIC-5 cells incubated with the S16A/P17A mutant virus were lower than those detected in the cells infected with WT virus (Fig. 2*g*, *upper panel, Sup.*). These results suggest that the infectivity defect of the S16A/P17A variant is linked to a dysfunction of the uncoating process.

Pin1 within the Target Cell Affects an Early Phase in HIV-1 Replication—Pin1 is a peptidyl-prolyl isomerase that specifically recognizes phosphorylated serine/threonine followed by proline via its WW domain and then catalyzes a conformational change of the bound substrate in a phosphorylation-dependent manner (24, 25). Pin1 has been shown to regulate the stability and localization of its substrates during transcriptional activation, cell cycle progression, and cell death, and a deregulated expression or loss of function of Pin1 leads to the progression of serious human diseases such as cancer and Alzheimer disease (24, 26–28). We therefore considered that Pin1 might bind to and regulate the function of the CA core. We first investigated whether Pin1 directly binds to the CA core by GST-Pin1 pulldown assay. Glutathione beads containing GST or GST-Pin1 were incubated with the CA core purified in accordance with the method described under "Experimental Procedures." To demonstrate that cores were indeed successfully purified, we performed a comparative immunoblot analysis of core preparations. As expected, the membrane-associated matrix (MA) protein (supplemental Fig. S2*a*) and the HIV surface glycoprotein gp120 (supplemental Fig. S2*b*) were substantially depleted in the core preparation. These results indicated that CA core is sufficiently purified. Therefore, in Pin1 pulldown assay, the binding proteins were then analyzed by immunoblotting with an anti-CA antibody. Fig. 3*a* shows that GST-Pin1, but not GST, was bound to the CA core. To investigate whether the binding of the CA core is directly due to the phosphorylation of Ser^{16} in the CA core, WT core particles were treated with ALP or the heat-denatured ALP. The treatment removed phosphate groups from phosphorylated Ser^{16} (Fig. 3*b*) and eliminated the Pin1 binding activity of the CA core (Fig. 3*c*). There are three highly conserved Ser-Pro motifs (Ser^{16}-Pro^{17}, Ser^{33}-Pro^{34}, and Ser^{146}-Pro^{147}) and a conserved Thr^{48}-Pro^{49} motif in the CA protein (supplemental Fig. S1). To examine whether Ser^{33}, Thr^{48}, or Ser^{146} in CA core is phosphorylated, the mixture of CA protein isoforms were subjected to proteome analysis (supplemental Fig. S3). The data demonstrated that Ser^{33}, Thr^{48}, and Ser^{146} in CA core were not phosphorylated. These results suggested that Pin1 binds preferentially to the phosphorylated Ser^{16}-Pro^{17} motif.

Because Pin1 has CA core binding activity, we next determined whether a decrease in endogenous Pin1 expression level decreases HIV-1 infectivity. We transfected MAGIC-5 cells

FIGURE 2. **The S16A/P17A CA mutant shows impaired uncoating process.** *a*, effect of various mutations in Ser^{16}-Pro^{17} motif on viral infectivity. Viral infectivity was determined using MAGIC-5 cells as previously described in Ref. 18. MAGIC-5 cells (1×10^4 cells) were exposed to an equal amount of WT or mutant viruses (corresponding to 3 ng RT). Statistical analysis using the analysis of variance test was performed. The *error bars* denote the standard deviation. *b*, replication kinetics of S16A/P17A variant in Jurkat and CEM cells. *c*, effect of alanine mutation of Ser^{16}-Pro^{17} motif on viral core phenotype. The *arrows* indicate electron-dense cores typical of intact HIV. *d*, effect of alanine mutation of Ser^{16}-Pro^{17} motif on viral entry efficiency. Viral entry assay was performed as described under "Experimental Procedures." *e* and *f*, quantitative analysis of HIV-1 reverse transcription during acute infection using early stage primers (*e*, R/U5) and late stage primers (*f*, R/gag). Briefly, MAGIC-5 cells (1×10^6 cells) were exposed to WT or S16A/P17A virus (2.5 ng of HIV-1 RT) and harvested at 1 day postinfection. The cells were washed with PBS(−), and nucleic acids were extracted. Quantitative analysis was performed using the same primers in accordance with the method of Ikeda *et al.* (17). The significant differences (unpaired *t* test) are indicated as follows: *, $p < 0.01$; *n.s.*, not significant. The *error bars* denote the standard deviation. *g*, effect of Ser^{16}-Pro^{17} motif on fate of CA core in infected cells. MAGIC-5 cells were incubated with WT HIV-1(VSV-G) or S16A/P17A HIV-1(VSV-G) at 4 °C for 30 min and then at 37 °C for 4 h. The cell lysates were analyzed as described under "Experimental Procedures." The supernatants and pellets were Western blotted for CA proteins.

with siRNA against Pin1 or control siRNA. As shown in the *top panel* of Fig. 3*d*, Pin1 siRNA (Pin1 C3) specifically decreased the Pin1 expression level in MAGIC-5 cells without altering actin or lactate dehydrogenase expression level. The cells were infected with HIV-1_{LAV-1}, and β-galactosidase activity was measured as an indicator of infection. In Fig. 3*e*, 60 nM Pin1 siRNA (Pin1 C3)-treated MAGIC-5 cells were infected with HIV-1_{LAV-1} (12 ng of p24 antigen) under the condition in which no HIV-1_{LAV-1}-induced CPE was observed in 60 nM control siRNA-treated MAGIC-5 cells. Interestingly, a decrease in endogenous Pin1 expression level decreased HIV-1_{LAV-1} infectivity (Fig. 3*e*, $p < 0.01$). Furthermore, the effects of Pin1-targeted siRNA treatment on HIV-1 replication were evaluated on the basis of cytopathic effect (*y*) observations (Fig. 3, *f–i*) and quantitative real time PCR analysis using primers designed to specifically amplify late products of reverse transcription. 60 nM

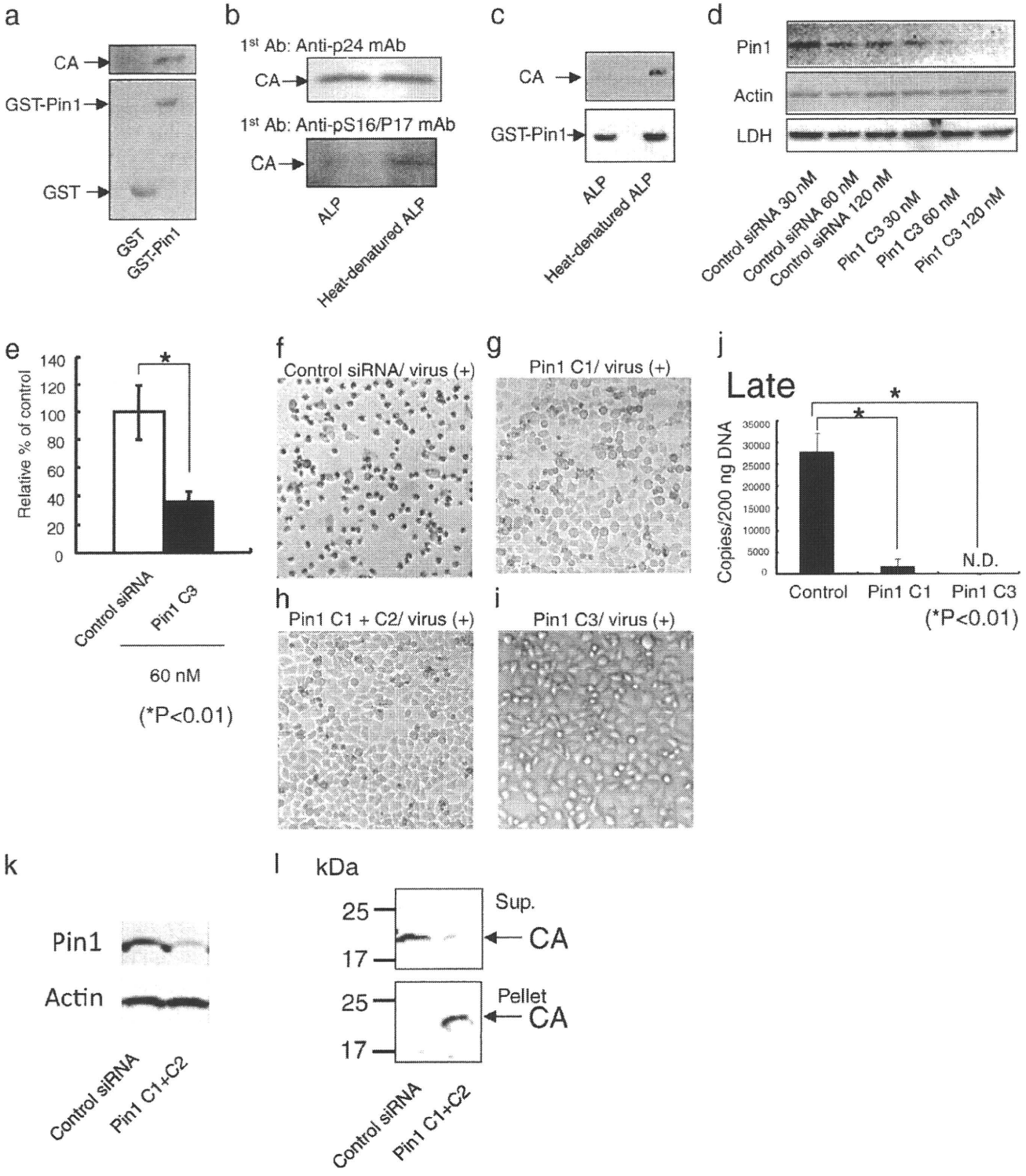

Pin1 C1-, C1+C2-, or C3-treated MAGIC-5 cells was infected with a single-round replication-defective HIV-1 under the condition in which a single-round replication-defective HIV-1-induced CPE was observed in 60 nM control siRNA-treated MAGIC-5 cells (Fig. 3, *f–i*). After treatment with siRNAs, MAGIC-5 cells were infected with single-round replication-defective $HIV_{NL4-3\Delta envWT}$ (11 ng of HIV RT). CPE in infected cells treated with the control siRNA was observed at 46 h postinfection (Fig. 3*f*). On the other hand, CPE was hardly observed in cells treated with 60 nM Pin1 C1, C1+C2, or C3 (Fig. 3, *g–i*, respectively). This indicates that Pin1-targeted siRNAs are capable of inhibiting CPE induced by HIV infection. Furthermore, Fig. 3*j* shows that there was a significant decrease in the level of the late (R/gag) form of the viral cDNA product.

To further examine whether Pin1 depletion is linked to a dysfunction of uncoating, cell-based fate-of-capsid uncoating assay was performed. The amounts of pelletable CA cores in the Pin1 knockdown cells infected with WT HIV-1(VSV-G) increased against those detected in the control siRNA-treated cells infected with WT HIV-1(VSV-G) (Fig. 3, *k* and *l*, *lower panels*, *Pellet*). Furthermore, the levels of the CA protein in the supernatants from the Pin1 knockdown cells infected with WT HIV-1(VSV-G) were lower than those detected in the control siRNA-treated cells infected with the WT HIV-1(VSV-G) (Fig. 3*l*, *upper panel*, *Sup.*). These results indicate that Pin1 depletion is linked to a dysfunction of uncoating.

Pin1 Induces Disassembly of the CA Core—Pin1 might regulate the uncoating of the CA core. To test this possibility, we attempted to study this process *in vitro* by detecting the disassembly of the CA core in the presence of Pin1. Purified CA cores were diluted with an uncoating assay buffer and incubated with GST-Pin1, heat-denatured, inhibitor-treated, or W34A/K63A GST-Pin1. Following incubation, the CA cores were subjected to ultracentrifugation to separate the free CA protein from the intact CA core. CA core dissociation was found to be GST-Pin1-dependent (Fig. 4*a*, *lane 2*), and the effect was attenuated when Pin1 was denatured (Fig. 4*b*, $p < 0.01$) or treated with the Pin1 inhibitor juglone (Fig. 4*c*, $p < 0.01$) and catalytically inactived the W34A/K63A Pin1 mutant (Fig. 4*d*, $p < 0.01$). Furthermore, the uncoating assay demonstrated that the Pin1-dependent disassembly was competed with the anti-pS16/P17 serum (Fig. 4*e*, $p < 0.01$) and blocked by the pretreatment of the core with ALP (Fig. 4*e*, $p < 0.01$). These results support the idea that Pin1 facilitates the HIV-1 uncoating by interacting with the CA core.

DISCUSSION

Much is known about the structure of the HIV-1 CA protein (29–31), but the mechanism and requirement of HIV-1 uncoating in postentry events have remained poorly defined. However, recent studies showed that the HIV-1 uncoating activity, which releases the CA protein from HIV-1 cores and is required for the activation of reverse transcriptase, is due to cellular factors (3, 4). The studies suggest that the ordered uncoating process of HIV-1 is not spontaneous and is regulated by cellular factors. Therefore, we employed a series of biochemical approaches to clarify the mechanism of HIV-1 CA core uncoating.

In this study, we showed that Pin1 assists the uncoating of the HIV core. Proteome analysis suggests that the Ser residue in the Ser^{16}-Pro^{17} motif of CA-a is preferentially phosphorylated (Fig. 1, *c* and *d*). Interestingly, three Ser-Pro motifs (Ser^{16}-Pro^{17}, Ser^{33}-Pro^{34}, and Ser^{146}-Pro^{147}) are highly conserved across HIV-1 clades (supplemental Fig. S1), and only the Ser^{16}-Pro^{17} motif is conserved among HIV-1, HIV-2, and simian immunodeficiency virus (SIV) (supplemental Fig. S4). As shown in Figs. 2*g* and 3*l*, cell-based fate-of-capsid uncoating assay demonstrated that the infectivity defect of the S16A/P17A variant is linked to a dysfunction of the uncoating process, and Pin1 depletion in the target cells is linked to a dysfunction of uncoating. Furthermore, GST-Pin1 pulldown assay and *in vitro* uncoating assay indicated that Pin1 facilitates HIV-1 uncoating by interacting with the CA core through the Ser^{16}-Pro^{17} motif (Figs. 3, *b* and *c*, and 4, *e* and *f*). These results suggest that only a fraction of the CA protein phosphorylated at Ser^{16}-Pro^{17} motif serves as a molecular switch to signal CA core uncoating because both the assembly and disassembly pathways cannot act on the CA core at the same time.

To investigate how the motif of CA-a is phosphorylated, Western immunoblot analysis with monoclonal anti-pS16/P17 mAb was carried out, which demonstrated that Ser^{16} was phosphorylated inside $HIV\text{-}1_{LAV\text{-}1}$ virions but not inside CEM/LAV-1 cells, although the specific kinase that phosphorylates Ser^{16} is currently unknown (supplemental Fig. S5). As shown in Fig. 3*e*, a decrease in endogenous Pin1 expression level decreases HIV-1 infectivity. These findings suggest that the CA

FIGURE 3. **Interactions of Pin1 with the CA core and Pin1 within the target cells regulate HIV-1 infectivity.** *a*, the CA core was subjected to GST-Pin1 pulldown assay and immunoblotted with anti-p24 mAb (*upper panel*). CBB staining of GST and GST-Pin1 (*lower panel*). *b*, treatment of CA core with ALP or heat-denatured ALP. The ALP- and heat-denatured ALP-treated CA cores were subjected to Western immunoblot analysis using anti-pS16/P17 mAb or anti-p24 mAb. The treatment removed phosphate groups from phosphorylated Ser^{16}. *c*, effect of ALP on interaction between Pin and CA core. The ALP-treated CA core was subjected to GST-Pin1 pulldown assay and immunoblotted with anti-p24 mAb (*upper panel*). CBB staining of GST-Pin1 is shown (*lower panel*). *d* and *e*, the suppression of Pin1 expression by 60 nM Pin1 C3 siRNA (*d*, *upper panel*, the expressions of actin and lactate dehydrogenase (*LDH*) were not affected by Pin1-specific siRNA)) in MAGIC-5 cells (1×10^4 cells) results in an attenuated $HIV\text{-}1_{LAV\text{-}1}$ replication (*e*). The significant differences (unpaired *t* test) are indicated as follows: *, $p < 0.01$. The *error bars* denote the standard deviation. *f–i*, the effects of Pin1-specific siRNAs were evaluated on the basis of CPE observations. The cells (2×10^5 cells) were pretreated with 60 nM control siRNA (*f*), Pin1 C1 (*g*), Pin1 C1+C2 (*h*), and Pin1 C3 (*i*) and then infected with single-round replication-defective HIV-1 ($HIV_{NL4-3\Delta envWT}$). Pin1-specific siRNAs were capable of inhibiting CPE induced by HIV infection. *j*, effect of Pin1 siRNAs on reverse transcription. The knockdown of Pin1 showed that there was a significant decrease in the level of the late (R/gag) form of the viral cDNA product. Statistical analysis using the analysis of variance test was performed. The *error bars* denote the standard deviation. *N.D.*, not detected. The detection limit of late products of HIV-1 reverse transcription was 400 copies/reaction in the assay. *k*, Pin1 C1+C2-induced suppression of Pin1 expression. MAGIC-5 cells were transfected with Pin1 C1+C2 siRNA (600 nM) using the Neon™ transfection system (*upper panel*, the expression of actin was not affected by Pin1 C1+C2). *l*, effect of Pin1 depletion on fate of CA core in infected cells. Pin1 knockdown cells treated with Pin1 C1+C2 siRNA were incubated with WT HIV-1(VSV-G) at 4 °C for 30 min and then at 37 °C for 4 h. The cell lysates were analyzed as described under "Experimental Procedures." The supernatants and pellets were analyzed by Western blotting for the CA proteins.

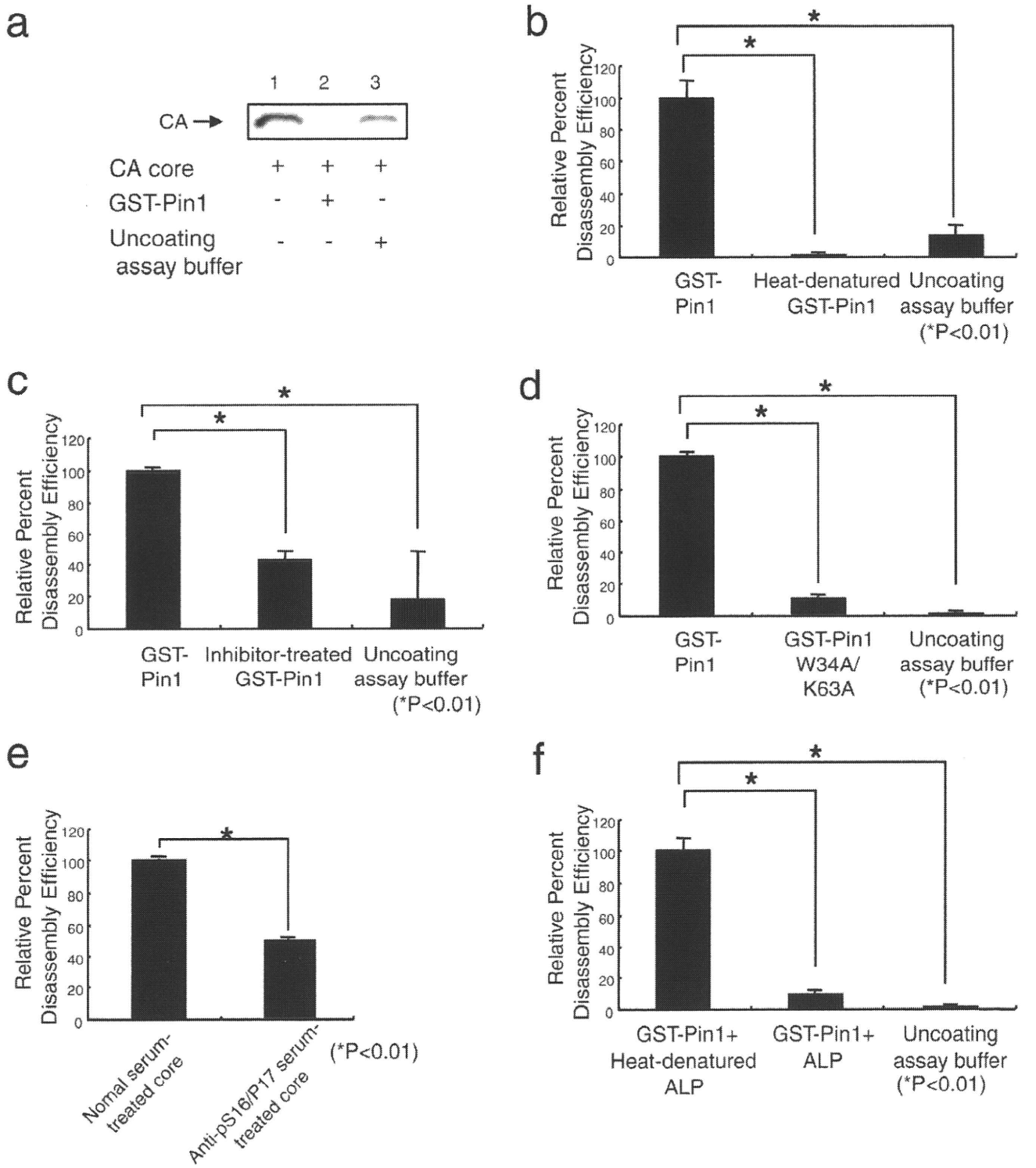

FIGURE 4. ***In vitro* uncoating of CA core by GST-Pin1.** *a*, *in vitro* uncoating assay was performed as described under "Experimental Procedures." The extent of uncoating was visualized by Western blot analysis using anti-p24 mAb after the undisassembled cores have been pelleted in an ultracentrifuge. CA cores in the presence of GST-Pin1 disassembled *in vitro* (*lane 2*). The quantities of the CA protein in the pellets in the presence of uncoating assay buffer were similar to that of the input CA protein (*lanes 1* and *3*). *b*, after incubating HIV-1 cores with GST-Pin1, heat-denatured GST-Pin1, or uncoating assay buffer for 1 h, the relative percentage of disassembly efficiency is given by the equation shown under "Experimental Procedures." Pin1 induces disassembly of the CA cores. *c*, *in vitro* uncoating activities after incubating HIV-1 cores with juglone-treated Pin1 for 1 h. The treatment of GST-Pin1 with juglone results in an attenuated *in vitro* uncoating. *d*, effect of GST-Pin1 (W34A/K63A) on uncoating. *In vitro* uncoating activities after incubating GST-Pin1 (W34A/K63A) with CA cores for 1 h. *e*, *in vitro* competitive uncoating assay. The pretreatment of CA cores with anti-pS16/p17 serum results in an attenuated *in vitro* uncoating. *f*, *in vitro* uncoating activities after incubating HIV CA cores with ALP for 2 h. Pin1-dependent disassembly was blocked by the pretreatment of the cores with ALP. *b–f*, statistical analysis using the analysis of variance test was performed. The *error bars* denote the standard deviation. The significant differences are indicated as follows: *, $p < 0.01$.

core phosphorylated inside the viral particle after release from the infected cells associates directly with Pin1 after entry into host cells for the uncoating process. A better understanding of these findings is crucial not only for elucidating the uncoating process at the early stage of the HIV-1 life cycle but also for identifying new anti-HIV drugs.

Acknowledgments—We thank A. Muneoka (Shin Nippon Biomedical Laboratories, Ltd.) for the technical support during electron microscopy. We thank Dr. R. Swanstrom (Lineberger Comprehensive Cancer Center, University of North Carolina at Chapel Hill) for support in preparing pNL4-3Δenv(S16A/P17A) with the pNL4-3-based env expression vector and helpful discussions.

REFERENCES

1. Goff, S. P. (2001) *J. Gene Med.* **3,** 517–528
2. Dvorin, J. D., and Malim, M. H. (2003) *Curr. Top. Microbiol. Immunol.* **281,** 179–208
3. Auewarakul, P., Wacharapornin, P., Srichatrapimuk, S., Chutipongtanate, S., and Puthavathana, P. (2005) *Virology* **337,** 93–101
4. Warrilow, D., Meredith, L., Davis, A., Burrell, C., Li, P., and Harrich, D. (2008) *J. Virol.* **82,** 1425–1437
5. Zack, J. A., Arrigo, S. J., Weitsman, S. R., Go, A. S., Haislip, A., and Chen, I. S. (1990) *Cell* **61,** 213–222
6. Stevenson, M., Stanwick, T. L., Dempsey, M. P., and Lamonica, C. A. (1990) *EMBO J.* **9,** 1551–1560
7. Misumi, S., Fuchigami, T., Takamune, N., Takahashi, I., Takama, M., and Shoji, S. (2002) *J. Virol.* **76,** 10000–10008
8. Veronese, F. D., Copeland, T. D., Oroszlan, S., Gallo, R. C., and Sarngadharan, M. G. (1988) *J. Virol.* **62,** 795–801
9. Mervis, R. J., Ahmad, N., Lillehoj, E. P., Raum, M. G., Salazar, F. H., Chan, H. W., and Venkatesan, S. (1988) *J. Virol.* **62,** 3993–4002
10. Macaulay, C., Meier, E., and Forbes, D. J. (1995) *J. Biol. Chem.* **270,** 254–262
11. Favreau, C., Worman, H. J., Wozniak, R. W., Frappier, T., and Courvalin, J. C. (1996) *Biochemistry* **35,** 8035–8044
12. Glavy, J. S., Krutchinsky, A. N., Cristea, I. M., Berke, I. C., Boehmer, T., Blobel, G., and Chait, B. T. (2007) *Proc. Natl. Acad. Sci. U.S.A.* **104,** 3811–3816
13. Ott, D. E., Coren, L. V., Kane, B. P., Busch, L. K., Johnson, D. G., Sowder, R. C., 2nd, Chertova, E. N., Arthur, L. O., and Henderson, L. E. (1996) *J. Virol.* **70,** 7734–7743
14. Adachi, A., Gendelman, H. E., Koenig, S., Folks, T., Willey, R., Rabson, A., and Martin, M. A. (1986) *J. Virol.* **59,** 284–291
15. O'Farrell, P. H. (1975) *J. Biol. Chem.* **250,** 4007–4021
16. Kawano, Y., Tanaka, Y., Misawa, N., Tanaka, R., Kira, J. I., Kimura, T., Fukushi, M., Sano, K., Goto, T., Nakai, M., Kobayashi, T., Yamamoto, N., and Koyanagi, Y. (1997) *J. Virol.* **71,** 8456–8466
17. Ikeda, T., Nishitsuji, H., Zhou, X., Nara, N., Ohashi, T., Kannagi, M., and Masuda, T. (2004) *J. Virol.* **78,** 11563–11573
18. Hachiya, A., Aizawa-Matsuoka, S., Tanaka, M., Takahashi, Y., Ida, S., Gatanaga, H., Hirabayashi, Y., Kojima, A., Tatsumi, M., and Oka, S. (2001) *Antimicrob. Agents Chemother.* **45,** 495–501
19. Stremlau, M., Perron, M., Lee, M., Li, Y., Song, B., Javanbakht, H., Diaz-Griffero, F., Anderson, D. J., Sundquist, W. I., and Sodroski, J. (2006) *Proc. Natl. Acad. Sci. U.S.A.* **103,** 5514–5519
20. Yee, J. K., Miyanohara, A., LaPorte, P., Bouic, K., Burns, J. C., and Friedmann, T. (1994) *Proc. Natl. Acad. Sci. U.S.A.* **91,** 9564–9568
21. Shen, M., Stukenberg, P. T., Kirschner, M. W., and Lu, K. P. (1998) *Genes Dev.* **12,** 706–720
22. Laurent, A. G., Krust, B., Rey, M. A., Montagnier, L., and Hovanessian, A. G. (1989) *J. Virol.* **63,** 4074–4078
23. Fuchigami, T., Misumi, S., Takamune, N., Takahashi, I., Takama, M., and Shoji, S. (2002) *Biochem. Biophys. Res. Commun.* **293,** 1107–1113
24. Wulf, G., Finn, G., Suizu, F., and Lu, K. P. (2005) *Nat. Cell Biol.* **7,** 435–441
25. Lu, K. P., Hanes, S. D., and Hunter, T. (1996) *Nature* **380,** 544–547
26. Ryo, A., Nakamura, M., Wulf, G., Liou, Y. C., and Lu, K. P. (2001) *Nat. Cell Biol.* **3,** 793–801
27. Zacchi, P., Gostissa, M., Uchida, T., Salvagno, C., Avolio, F., Volinia, S., Ronai, Z., Blandino, G., Schneider, C., and Del Sal, G. (2002) *Nature* **419,** 853–857
28. Liou, Y. C., Sun, A., Ryo, A., Zhou, X. Z., Yu, Z. X., Huang, H. K., Uchida, T., Bronson, R., Bing, G., Li, X., Hunter, T., and Lu, K. P. (2003) *Nature* **424,** 556–561
29. Gamble, T. R., Vajdos, F. F., Yoo, S., Worthylake, D. K., Houseweart, M., Sundquist, W. I., and Hill, C. P. (1996) *Cell* **87,** 1285–1294
30. Gamble, T. R., Yoo, S., Vajdos, F. F., von Schwedler, U. K., Worthylake, D. K., Wang, H., McCutcheon, J. P., Sundquist, W. I., and Hill, C. P. (1997) *Science* **278,** 849–853
31. Gitti, R. K., Lee, B. M., Walker, J., Summers, M. F., Yoo, S., and Sundquist, W. I. (1996) *Science* **273,** 231–235

Suppression of Human Immunodeficiency Virus Type-1 Production by Coexpression of Catalytic-Region-Deleted *N*-Myristoyltransferase Mutants

Nobutoki TAKAMUNE,*[a] Tetsuya KUROE,[a] Noriaki TANADA,[a] Shozo SHOJI,[a,b] and Shogo MISUMI[a]

[a] *Department of Pharmaceutical Biochemistry, Faculty of Life Sciences, Kumamoto University; 5–1 Oe-Honmachi, Kumamoto 862–0973, Japan: and* [b] *Kumamoto Health Science University; 325 Izumimachi, Kumamoto 861–5598, Japan.*
Received July 9, 2010; accepted October 6, 2010; published online October 6, 2010

_N_-Myristoyltransferase (NMT) isozymes, *i.e.*, NMT1 and NMT2, are essential host factors for the AIDS-causing human immunodeficiency virus type-1 (HIV-1), by which the viral proteins $Pr55^{gag}$ and Nef are _N_-myristoylated. _N_-Myristoylation is important for the membrane targeting of modified proteins. Since it is predicted that approximately 0.5% of all proteins in the human genome are _N_-myristoylated, selective inhibition of closely HIV-1-associated NMT isozymes is thought to be important for the improvement of specificity in the anti-HIV-1 strategy with the inhibition of NMT function. NMT isozymes contain two characteristic structures, the N-terminal region and the catalytic region. Here, it was shown that the N-terminal region of each NMT isozyme is required for isozyme-specific binding to the ribosome. The specific binding of each isozyme to the ribosome was associated with HIV-1 production, in which NMT1 and NMT2 in the ribosome were suggested to be mainly related to $Pr55^{gag}$ and Nef, respectively. These results indicate that the N-terminal region that mediates binding to the ribosome can become a target for NMT-isozyme-specific inhibition, which could block HIV-1 production.

Key words _N_-myristoyltransferase; ribosome; human immunodeficiency virus type-1; $Pr55^{gag}$; Nef; _N_-myristoylation

_N_-Myristoyltransferase (NMT) catalyzes the modification with myristic acid of N-terminal Gly of a number of proteins[1]; this modification is called protein _N_-myristoylation.[2] The consensus sequence of peptide substrates for NMT is known, in which N-terminal Gly at position two is absolutely required.[1,3] _N_-Myristoylation is important for the membrane targeting of modified proteins.

_N_-Myristoylation occurs cotranslationally[4] and post-translationally.[5] Cotranslational _N_-myristoylation usually occurs at Gly exposed after the removal of the initiator Met from the nascent peptide with the consensus sequence.[6] Post-translational _N_-myristoylation also occurs at Gly exposed in caspase-cleavaged proteins with the consensus sequence.[5] Many viral proteins in addition to cellular proteins are _N_-myristoylated.[6,7]

_N_-Myristoylation occurs in products from the AIDS-causing human immunodeficiency virus type-1 (HIV-1) genome; $Pr55^{gag}$[8] and Nef.[9] $Pr55^{gag}$ is a precursor form of structural proteins of HIV-1 and its _N_-myristoylation is essential for the production of virions.[8] Nef is an accessory protein of HIV-1 and its _N_-myristoylation is essential for its multiple functions leading to the enhancement of viral replication.[10]

In humans, NMT consists of multiple isozymes encoded by NMT1[11] and NMT2.[12] These NMT isozymes contain two characteristic structures, the N-terminal region and the catalytic region. The NMT1 family consists of a few isozymes with different lengths of the N-terminal region.[13] It has been suggested that each NMT isozyme has a specific role *in vivo*.[14,15] Additionally, siRNA using studies suggested that NMT1 and NMT2 are respectively associated with the membrane targeting of $Pr55^{gag}$ and Nef.[16,17]

In a previous study of the NMT1 isozyme, it was reported that the N-terminal region is not required for the catalytic activity[11] but is associated with ribosomal targeting.[18] However, it remains to be elucidated whether the N-terminal region differs in property in between NMT1 and NMT2. It was therefore hypothesized that the N-terminal region of each NMT isozyme is associated with a specific role of each NMT isozyme in the ribosome.

In this study, it was clarified that the N-terminal regions in both NMT isozymes are sufficient for binding to the ribosome, in which each basic-amino-acid-rich cluster sequence, named the K box, is essential for the binding. The catalytic region-deleted NMT mutants, NMTΔCs, affected the bindings of endogenous NMTs, which resulted in relative reduction of endogenous NMTs in ribosome fraction. Furthermore, the coexpression of NMTΔCs induced significant reduction of HIV-1 production. These results suggest that the bindings of endogenous NMTs to ribosome could be associated with effective HIV-1 production, which led us to hypothesize that such bindings can become a target for inhibition of HIV-1 replication.

MATERIALS AND METHODS

Materials The infectious HIV-1 expression vector pNL-CH was kindly gifted by Dr. Ron Swanstrom of the UNC Center for AIDS Research, University of North Carolina at Chapel Hill, Chapel Hill, NC. Dulbecco's modified Eagle's medium (DMEM) was gifted from Nissui Pharmaceutical Co., Ltd.

Construction of Each NMT Isozyme and Mutant Expression Vectors The expression vectors for the NMT1ΔC, NMT2ΔC, NMT2ΔCΔKbox, and NMT1LΔCΔKbox proteins, which are tagged with a V5 epitope at the C-terminus, were constructed using polymerase chain reaction (PCR) and standard subcloning techniques. The V5 epitope tag sequence is GKPIPNPLLGLDST, which is from V protein and phosphoprotein of simian virus 5. The PCR products coding NMT1ΔC and NMT2ΔC were subcloned into the pcDNA4/HisMax vector (Invitrogen, Carlsbad, CA, U.S.A.) for its expression in mammalian cells. NMT1ΔC- and

* To whom correspondence should be addressed. e-mail: tkmnnbtk@gpo.kumamoto-u-ac.jp

NMT2ΔC-coding DNAs without the K box region were amplified by PCR, followed by self-ligation. Full-length NMT1, NMT2, and their ΔKbox mutants, which were tagged with a Xpress epitope at the N-terminus, were also constructed as well.

Construction of Each HIV-1 Expression Vector A Gly^2-to-Ala^2 (G2A) mutation in *gag* and *nef* was introduced into the infectious molecular clone pNL-CH[19] derived from the pNL4-3 clone using the site-directed mutagenesis method. The mutant constructs were designated pNL-CH/gagG2A, pNL-CH/nefG2A and pNL-CH/gagG2A/nefG2A.

Preparation of Cytosolic and Ribosomal Fractions To separate the cytosolic fraction and the ribosomal fraction in the human embryonic kidney (HEK)293 cells used in the studies, the homogenates of the cells were subjected to subcellular fractionation using sequential differential centrifugation, as previously described.[18] To comparison of distribution of NMTs between ribosomal fraction and cytosolic fraction, same percentage of volume of each fraction was subjected to the western blot analysis.

Quantification of HIV-1 p24 Antigen in Supernatant Each NMT mutant protein expressing HEK293 cells (1.0×10^6 cells) were cultured in six-well plates overnight. Confluent cells (30—50%) were transfected with each HIV-1 expression vector (pNL-CH, pNL-CH/gagG2A, pNL-CH/nefG2A, and pNL-CH/gagG2A/nefG2A) using Lipofectamine™ LTX. After 48-h cultivation, the level of HIV-1 p24 antigen in the cell-free supernatant was measured using an enzyme-linked immunosorbent assay (ELISA) kit (ZeptoMetrix Corporation, Buffalo, NY, U.S.A.), according to the manufacturer's instruction.

Cell Lysis and Western Immunoblot Analysis The cells were washed, lysed and subjected to Western blot analysis.[16] The serum and antibodies used in different immunoblottings were as follows: anti-V5 (Invitrogen, Carlsbad, CA, U.S.A.), anti-lactate-dehydrogenase (Chemicon, Temecula, CA, U.S.A.), anti-NMT1 (BD Pharmingen, San Diego, CA, U.S.A.), and anti-NMT2 (BD Pharmingen, San Diego, CA, U.S.A.) antibodies. Immune complexes were detected with appropriate peroxidase-conjugated secondary antibodies followed by visualization by chemiluminescence detection (NEN Life Science Products, Boston, MA, U.S.A.).

RNA Extraction and Detection of 28S Ribosomal RNA (rRNA) Total RNA from each fraction was extracted using Isogen (NIPPON GENE Co., Ltd., Tokyo, Japan). The extracted RNA was subjected to agarose gel electrophoresis and stained with ethidium bromide.

RESULTS AND DISCUSSION

The details of catalytic region of NMT have been well understood, in which there are the binding sites for myristoyl-CoA and peptide substrate.[20] On the other hand, the N-terminal region of NMT remains to be elucidated. Figure 1A illustrates that the NMT isozymes consist of an N-terminal region and a catalytic region, except for NMT1 short form (NMT1S) that contains no N-terminal region. It has not been confirmed whether endogenous NMT1 and endogenous NMT2 could actually localize to ribosome in addition to cytosol. Hence, the subcellular localization of endogenous NMT isozymes in HEK293 cells was analyzed using anti-NMT1 and NMT2 antibodies. Lactate dehydrogenase (LDH) and 28S ribosomal RNA were detected as cytosolic and ribosomal markers, respectively. As shown in Fig. 1B, NMT1 and NMT2 were detected in both cytosolic and ribosomal fractions; on the other hand, NMT1S was detected in only the cytosolic fraction. It was confirmed that endogenous NMT isozymes with the N-terminal region localize to the ribosome in addition to the cytosol, suggesting that N-terminal regions are associated with ribosomal targeting.

The N-terminal region has been suggested to be responsible for the ribosomal targeting of both NMT isozymes. Additionally, note that a unique sequence exists within the N-terminal region of each NMT isozyme, which consists of a basic-amino-acid-rich cluster sequence, named K box (Fig. 1A). To determine whether each N-terminal region is sufficient and whether the K box is important for ribosomal localization in both NMT isozymes, the ability of ribosomal localization of the catalytic-region-deleted NMT1 and NMT2 mutants with or without the K box (Fig. 2A) was examined. As shown in Fig. 2B, both NMT1ΔC and NMT2ΔC were detected in the both ribosomal and cytosolic fractions,

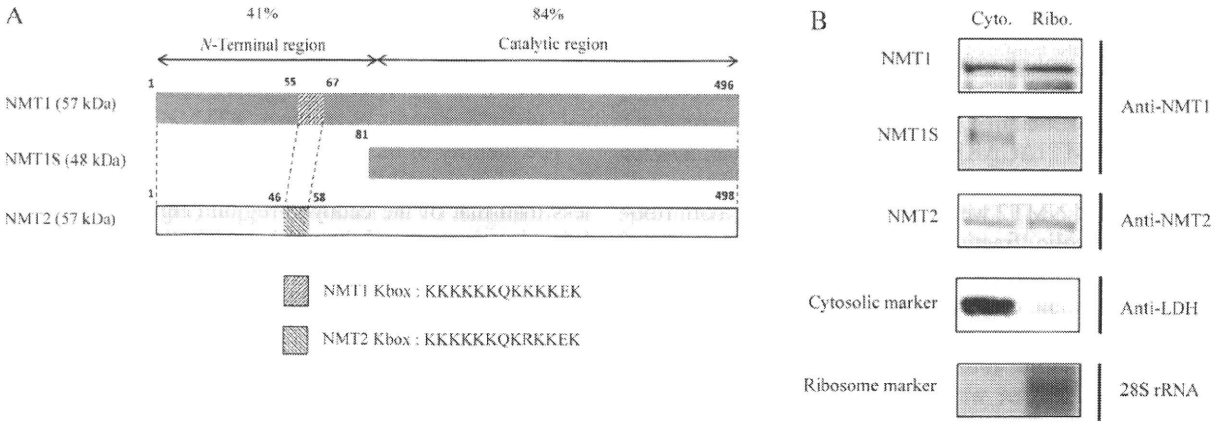

Fig. 1. Detection of Endogenous NMT Isozymes in Ribosomal and Cytosolic Fractions

(A) Schematic of each NMT isozyme and K box amino acid sequences. The percentages represent identities between NMT1 and NMT2. (B) The ribosomal and cytosolic fractions were isolated from HEK293 cells by differential centrifugation. The fractions were subjected to Western blot analysis using anti-NMT1 and anti-NMT2 antibodies. LDH was detected using a specific antibody as the cytosolic marker. RNA was isolated from the fractions and subjected to agarose electrophoresis, and stained with ethidium bromide. Cyto., cytosol fraction; Ribo., ribosomal fraction.

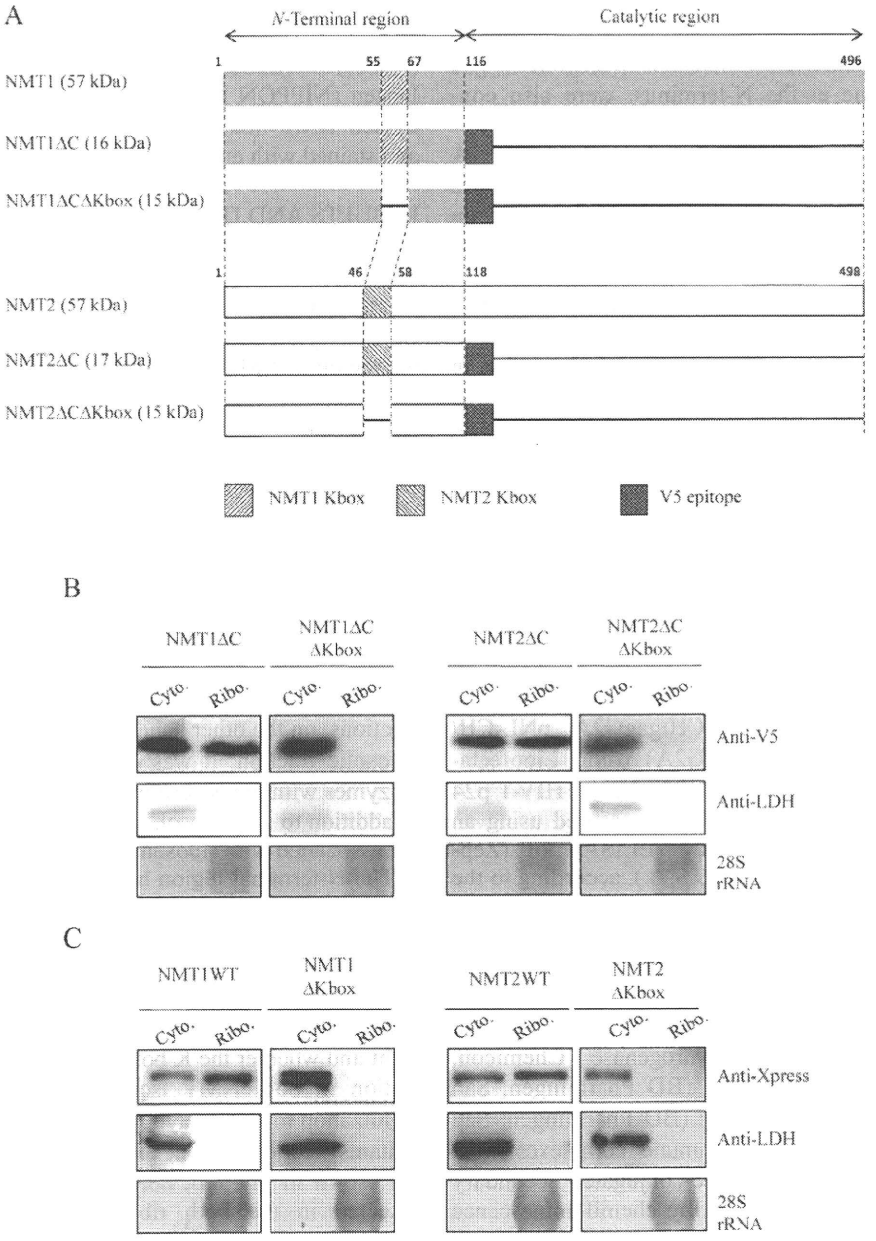

Fig. 2. Distributions in Ribosome and Cytosol of NMTΔC Mutants with or without K Box

Schematic representation of mutated NMT constructs used in the study (A). HEK293 cells were transfected with DNA for NMT1ΔC, NMT2ΔC, NMT1ΔCΔK, or NMT2ΔCΔK (B). HEK293 cells were also transfected with DNA for NMT1, NMT2, NMT1ΔK, or NMT2ΔK (C). Forty-eight hours post-transfection, the cells were lysed and subjected to subcellular fractionation to isolate the ribosomal and cytosolic fractions, followed by Western blot analysis to detect the NMT mutants, as described in Fig. 1.

whereas both NMT1ΔCΔKbox and NMT2ΔCΔKbox were detected in only the cytosolic fraction. Both exogenous full length NMT1 and NMT2 were also detected in the both ribosomal and cytosolic fractions, in which the amounts of NMT1 and NMT2 in ribosomal fractions were relatively higher than those in cytosolic fractions. The results were identical to the endogenous NMT1 and NMT2 distribution. It was also shown that the ability of distribution to ribosome of each full-length isozyme was lost by deletion of the K box (Fig. 2C), which results were identical to the distributions of the NMT1ΔCΔKbox and NMT2ΔCΔKbox (Fig. 2B). The results indicate that the N-terminal region is sufficient and the K box is required for the ribosomal localization in both NMT1 and NMT2.

The identity of the amino acid sequence of the N-terminal region between NMT1 and NMT2 is 41%, which is much less than that of the catalytic region (Fig. 1A). Additionally, it has been suggested that each NMT isozyme has a specific role *in vivo*.[14—17] We therefore hypothesized that the lower identity of the N-terminal region between NMT1 and NMT2 is associated with the specific role of each isozyme at the ribosome. It was then examined whether the expressions of NMT1ΔC and NMT2ΔC can affect the ribosomal localization of endogenous NMT1 and NMT2. After subcellular fractionation, the endogenous NMT1 and NMT2 were detected by western immunoblot analysis using each NMT antibody as described in Materials and Methods. Since molecular weights of endogenous NMTs and NMTΔC mutants

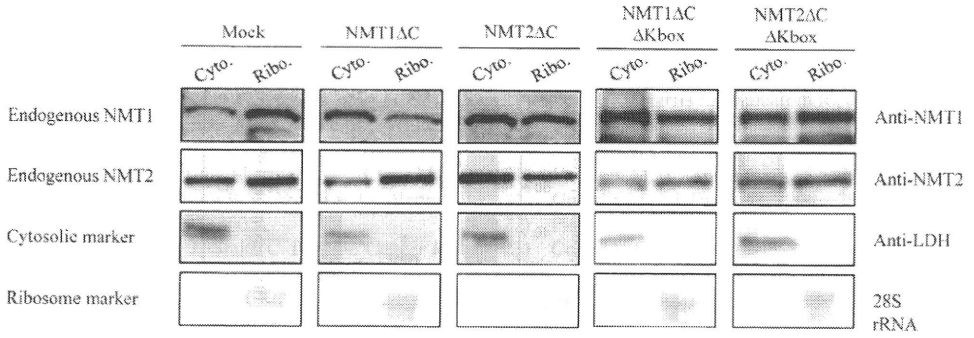

Fig. 3. Effect of NMT Mutants on Each Endogenous NMT Isozyme in Ribosome

The ribosomal and cytosolic fractions were isolated from HEK293 cells expressing NMT1ΔC, NMT2ΔC, NMT1ΔCΔK, or NMT2ΔCΔK. Each endogenous NMT isozyme in both fractions was detected by Western blot analysis, as described in Fig. 1.

were 57 kDa and 16—17 kDa, respectively, it could be distinguished between the endogenous NMTs and the mutants in the western blot analysis using each anti-NMT isozyme specific antibody. As shown in the result of the mock transfected HEK293 cells in Fig. 3, the amounts of endogenous NMT isozymes in the ribosomal fraction were relatively larger than those in the cytosolic fraction. The amount of endogenous NMT1 in the ribosomal fraction relatively decreased with the expression of NMT1ΔC. The expression of NMT2ΔC was also associated with partial decrease of the relative amount of endogenous NMT1 in ribosomal fraction; on the other hand, the amount of endogenous NMT2 in the ribosomal fraction relatively decreased with the expression of NMT2ΔC but not of NMT1ΔC. Additionally, no effect of NMT1ΔCΔK or NMT2ΔCΔK, which exclusively localizes in the cytosol, on the ribosomal localization of endogenous NMT isozymes was observed (Fig. 3). The results suggest that NMT1ΔC and NMT2ΔC compete with endogenous NMT1 and endogenous NMT2 for the binding to the ribosome, respectively.

Taken together, the K box is thought to be essential for the binding of NMT1 and NMT2 to the ribosome, whereas the N-terminal region except the K box, which shows a low identity between NMT1 and NMT2, may contribute to the specific binding of each isozyme to the ribosome. While NMTDC mutants could bind to ribosome mediated by the K box, endogenous NMTs could bind to ribosome mediated by not only the K box but also interaction between catalytic region and N-terminal peptide of substrate protein under synthesis on the ribosome. Taking this possibility to consideration, the affinity of NMTDC mutants to ribosome might not be comparable to that of the endogenous NMTs.

We confirmed the importance of the *N*-myristoylation of $Pr55^{gag}$[8] and Nef[21] for the production of HIV-1 virions from HEK293 cells. As shown in Fig. 4A, the level of viral production from HEK293 cells transfected with proviral DNA for HIV-1 with a G2A mutation in the N-terminus of $Pr55^{gag}$ (gagG2A) or Nef (nefG2A) was about 20% or 50% of that of the HIV-1 wild type (WT). Furthermore, the level of production of HIV-1 with G2A mutations in both $Pr55^{gag}$ and Nef (gagG2A/nefG2A) was similar to that of HIV-1 gagG2A. The effect of gagG2A on the reduction in the level of viral production was stronger than that of nefG2A.

siRNA using studies have suggested that NMT1 and NMT2 are at least closely associated with $Pr55^{gag}$ and Nef, respectively, in HIV-1 replication.[16,17] In other words, these results indicate that the production of HIV-1 WT depends on both NMT1 and NMT2, whereas the production of HIV-1 nefG2A depends on mainly NMT1. Since the competition of NMT1ΔC and NMT2ΔC with endogenous NMT isozymes for the targeting to the ribosome showed isozyme specificity (Fig. 3), we asked whether the each mutant could also affect the HIV-1 production mediated by each endogenous ribosomal NMT isozyme. To address this question, HEK293 cells expressed with or without NMT1ΔC or NMT2ΔC were transfected with proviral DNA for HIV-1 WT or HIV-1 nefG2A and the level of viral production in the supernatant was measured. As shown in Figs. 4B and C, the level of HIV-1 WT production significantly decreased with the expression of either NMT1ΔC or NMT2ΔC, compared with that of the control. The level of HIV-1 nefG2A production significantly decreased with the expression of NMT1ΔC, which reduction level was similar to the case of HIV-1 WT. On the other hand, the effect of expression of NMT2ΔC on reduction of HIV-1 nefG2A production was less than that of HIV-1 WT. The results suggest that the production of HIV-1 WT is associated with both NMT1 and NMT2, whereas the production of HIV-1 nefG2A is mainly associated with NMT1, whose relations were similar to the that in the case of siRNA using previous studies.[16,17]

Almost no effects of coexpression of NMT1ΔC or NMT2ΔC on productions of HIV-1 gagG2A and HIV-1 gagG2A/nefG2A were expectedly observed (Figs. 4D, E), which viruses have essentially extreme low production competence due to non *N*-myristoylation of $Pr55^{gag}$ (Fig. 4A). The expression of each NMTΔC mutant in each case was verified by western blot analysis (Fig. 4D).

Altogether, it is thought that NMT1ΔC or NMT2ΔC specifically affects endogenous NMT1 or NMT2 by the competition of the binding site on the ribosome, which might lead to miss the cotranslational *N*-myristoylation of the nascent peptides of $Pr55^{gag}$ by NMT1 or Nef by NMT2 in the ribosome, although it has not been confirmed whether the *N*-myristoylation of $Pr55^{gag}$ or Nef is actually affected. Alternatively, it is also thought that the NMTΔC mutants might affect the viral production mediated by host *N*-myristoyl proteins.

In current HIV-1 therapy, the appearance of drug resistant HIV-1 is a serious problem.[22] One of the fundamental reasons is the targeting of viral factors. It has therefore been

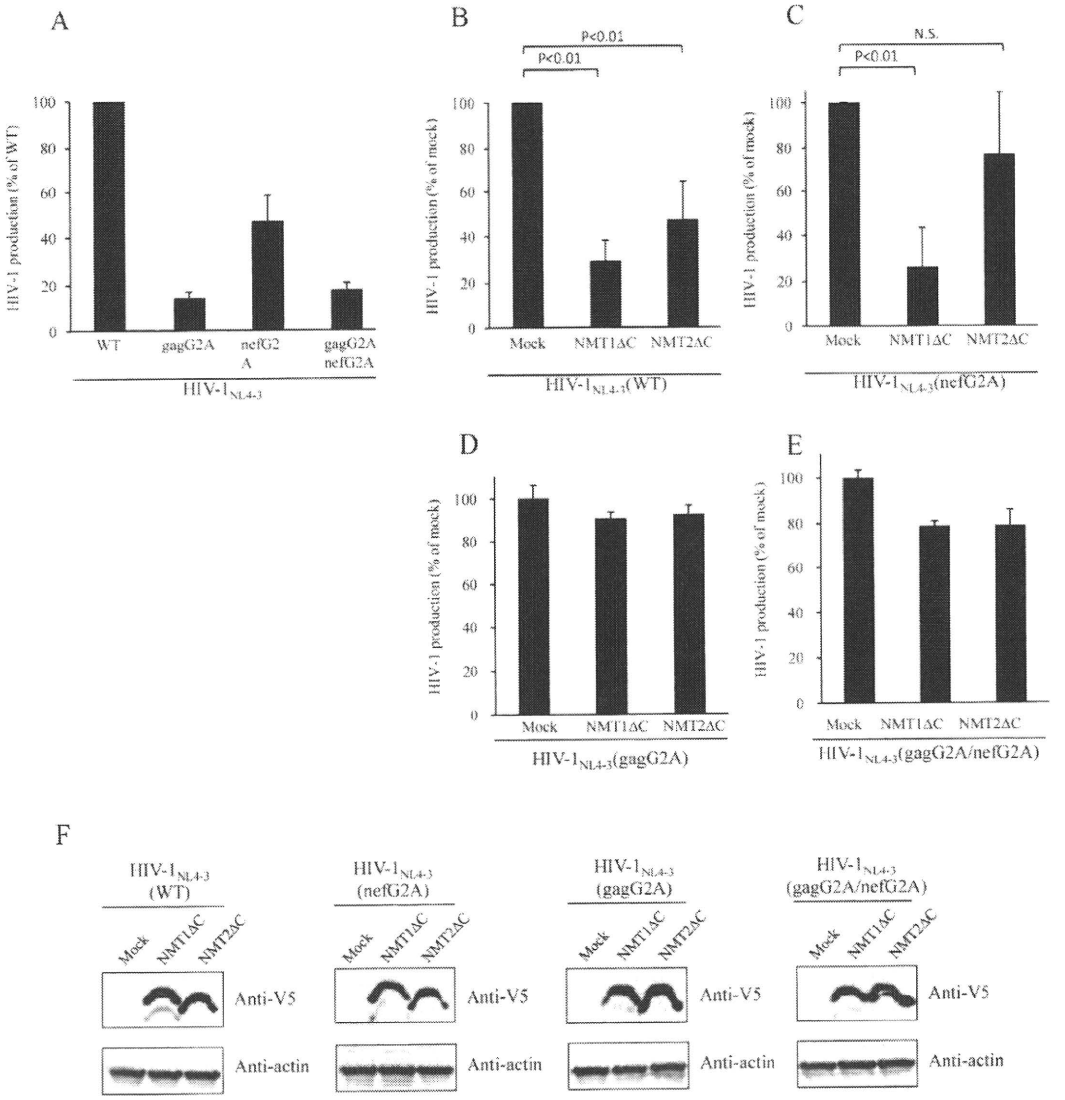

Fig. 4. Effect of NMT Mutants on WT and Nef-deficient HIV-1 Productions

HEK293 cells were transfected with proviral DNA for HIV-1 WT, HIV-1 gagG2A, HIV-1 nefG2A, or HIV-1 gagG2A/nefG2A. Forty-eight hours post-transfection, the level of virus production in the supernatant was measured by p24 ELISA (A). HEK293 cells expressing NMT1ΔC, NMT2ΔC, or a mock vector were transfected with proviral DNA for HIV-1 WT (B), HIV-1 nefG2A (C), HIV-1 gagG2A (D), or HIV-1 gagG2A/nefG2A (E). Forty-eight hours post-transfection, the level of virus production in the supernatant was measured by p24 ELISA. NMTΔC mutants and actin were detected by Western blot analysis (F). Each bar represents the mean standard deviation (n=3). * p was calculated using Welch's t-test. N.S.: not significant.

proposed that the host factors required for HIV-1 replication could also become potential therapeutic targets.[23] The *N*-myristoylation of both $Pr55^{gag}$ and Nef is almost completely conserved in extremely diverse HIV-1, suggesting that the inhibition of NMT, especially the $Pr55^{gag}$-associated ribosomal NMT1 isozyme, is one of the most attractive targets against HIV-1. Since it is predicted that approximately 0.5% of all proteins in the human genome are *N*-myristoylated,[24] it should be investigated how the inhibition of targeting of NMT to ribosome could affect the other host *N*-myristoylated proteins, for example *src* family kinases and small G proteins. To accomplish such a strategy, the specific blockage of NMT isozyme targeting to the ribosome could become a novel therapeutic strategy for HIV-1 diseases.

Acknowledgements This study was supported in part by Grants-in-Aid for Young Scientists from the Ministry of Education, Culture, Sports, Science and Technology of Japan and a Health and Labour Sciences Research Grants from Ministry of Health, Labour and Welfare of Japan.

REFERENCES

1) Towler D. A., Adams S. P., Eubanks S. R., Towery D. S., Jackson-Machelski E., Glaser L., Gordon J. I., *J. Biol. Chem.*, **263**, 1784—1790 (1988).
2) Carr S. A., Biemann K., Shoji S., Parmelee D. C., Titani K., *Proc. Natl. Acad. Sci. U.S.A.*, **79**, 6128—6131 (1982).
3) Towler D., Glaser L., *Proc. Natl. Acad. Sci. U.S.A.*, **83**, 2812—2816 (1986).
4) Wilcox C., Hu J. S., Olson E. N., *Science*, **238**, 1275—1278 (1987).
5) Zha J., Weiler S., Oh K. J., Wei M. C., Korsmeyer S. J., *Science*, **290**, 1761—1765 (2000).
6) Boutin J. A., *Cell Signal.*, **9**, 15—35 (1997).
7) Resh M. D., *Biochim. Biophys. Acta*, **1451**, 1—16 (1999).
8) Bryant M., Ratner L., *Proc. Natl. Acad. Sci. U.S.A.*, **87**, 523—527 (1990).
9) Guy B., Kieny M. P., Riviere Y., Le Peuch C., Dott K., Girard M., Montagnier L., Lecocq J. P., *Nature* (London), **330**, 266—269 (1987).

10) Fackler O. T., Moris A., Tibroni N., Giese S. I., Glass B., Schwartz O., Krausslich H. G., *Virology*, **351**, 322—339 (2006).
11) Duronio R. J., Reed S. I., Gordon J. I., *Proc. Natl. Acad. Sci. U.S.A.*, **89**, 4129—4133 (1992).
12) Giang D. K., Cravatt B. F., *J. Biol. Chem.*, **273**, 6595—6598 (1998).
13) McIlhinney R. A., Young K., Egerton M., Camble R., White A., Soloviev M., *Biochem. J.*, **333**, 491—495 (1998).
14) Yang S. H., Shrivastav A., Kosinski C., Sharma R. K., Chen M. H., Berthiaume L. G., Peters L. L., Chuang P. T., Young S. G., Bergo M. O., *J. Biol. Chem.*, **280**, 18990—18995 (2005).
15) Ducker C. E., Upson J. J., French K. J., Smith C. D., *Mol. Cancer Res.*, **3**, 463—476 (2005).
16) Takamune N., Gota K., Misumi S., Tanaka K., Okinaka S., Shoji S., *Microbes. Infect.*, **10**, 143—150 (2008).
17) Seaton K. E., Smith C. D., *J. Gen. Virol.*, **89**, 288—296 (2008).
18) Glover C. J., Hartman K. D., Felsted R. L., *J. Biol. Chem.*, **272**, 28680—28689 (1997).
19) Lee S. K., Harris J., Swanstrom R., *J. Virol.*, **83**, 8536—8543 (2009).
20) Maurer-Stroh S., Eisenhaber B., Eisenhaber F., *J. Mol. Biol.*, **317**, 523—540 (2002).
21) Chowers M. Y., Spina C. A., Kwoh T. J., Fitch N. J., Richman D. D., Guatelli J. C., *J. Virol.*, **68**, 2906—2914 (1994).
22) Flexner C., *Nat. Rev. Drug Discov.*, **6**, 959—966 (2007).
23) Cohen J., *Science*, **319**, 143—144 (2008).
24) Maurer-Stroh S., Eisenhaber B., Eisenhaber F., *J. Mol. Biol.*, **317**, 541—557 (2002).